

An overview of $\eta_c(1S)$, $\eta_c(2S)$ and $h_c(1P)$ physics at BESIII

Q. P. Ji^{a*}

Henan Normal University, Xinxiang 453007, China

S. S. Fang^{b†} and Z. Y. Wang^{b‡}

Institute of High Energy Physics, Chinese Academy of Science, Beijing 100049, China

(Dated: August 31, 2021)

The three singlet charmonium states, i.e., $\eta_c(1S)$, $\eta_c(2S)$ and $h_c(1P)$, composed of $c\bar{c}$ pairs and below the $D\bar{D}$ threshold, provide a good platform for the researches in understanding Quantum Chromodynamics (QCD). While they can not be produced directly in e^+e^- annihilation. The resulting limited statistics and photon-detection challenges also are major obstacles to the researches of their properties. Here we review BESIII results involving $\eta_c(1S)$, $\eta_c(2S)$ and $h_c(1P)$ so far, including measurements for their resonance parameters, the first observation of $M1$ transition $\psi(2S) \rightarrow \gamma\eta_c(2S)$, as well as the measurement for the $h_c(1P)$ hadronic and radiative decays, and so on. The prospects for further research on these three states at BESIII are also presented.

PACS numbers: 13.20.Pq, 13.25.Gv, 12.38.Qk

I. INTRODUCTION

Since the discovery of the $J/\psi(1S)$ more than 40 years ago, a lot of charmonium states composed of $c\bar{c}$ are well established (c denotes the charmed quark, and \bar{c} for charmed antiquark). The corresponding low-lying charmonium $c\bar{c}$ spectrum with selected decay modes and transition is shown in Fig. 1. The levels are labeled by S , P , D , corresponding to relative orbital angular momentum $L = 0, 1, 2$ between c and \bar{c} . The spin of the c and \bar{c} can be couple to either $S = 0$ (spin-singlet) or $S = 1$ (spin-triplet) states. The parity of a $c\bar{c}$ bound state with orbital angular momentum L is $P = (-1)^{L+1}$; the charge-conjugation eigenvalue is $C = (-1)^{L+S}$. Values of J^{PC} are shown at the bottom of the Fig. 1. States are often denoted by $^{2S+1}[L]_J$, with $[L] = S, P, D, \dots$. Thus $L = 0$ states can be 1S_0 or 3S_1 ; $L = 1$ states can be 1P_1 or $^3P_{0,1,2}$ and so on. The radial quantum number is denoted by n .

As the lowest-lying S -wave spin-singlet charmonium state, $\eta_c(1S)$, was discovered using the Crystal Ball NaI detector at SPEAR in 1980 [2], and radiative transitions to this state are observed from $\psi(2S)$ and J/ψ in the inclusive photon spectra. Although it has been known for about thirty years, the properties of this charmonium state are still under investigation. Especially when considering the available data on the branching fractions (BFs) of different decay modes of the $\eta_c(1S)$, it becomes obvious that this resonance is not fully understood yet. Several BFs are only measured roughly or with large uncertainties, and the observed BFs sum up to only about 57% [3]. Also the observed mass and decay width show a

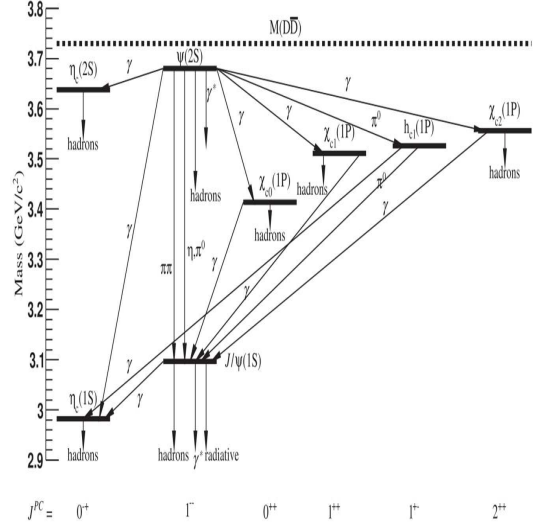


FIG. 1. Low-lying charmonium ($c\bar{c}$) spectrum, with selected decay modes and transition [1].

large variation from experiment to experiment, and may depend on the production, and/or decay process in which they are observed.

About two decades after the discovery of $\eta_c(1S)$, its first radial excited state, $\eta_c(2S)$, was first observed by the Belle collaboration in the process $B^\pm \rightarrow K^\pm\eta_c(2S)$ with $\eta_c(2S) \rightarrow K_S^0 K^\pm\pi^\mp$ [4], then confirmed in the two-photon production of $K_S^0 K^\pm\pi^\mp$ [5, 6] and $K^+K^-\pi^+\pi^-\pi^0$ [7], as well as in the double-charmonium production process $e^+e^- \rightarrow J/\psi c\bar{c}$ [8, 9]. Combining the world average values from PDG 2012 [10], with the results from Belle and BABAR on two-photon fusion into hadronic final states other than $K_S^0 K^\pm\pi^\mp$ [7], one obtains updated averages of the $\eta_c(2S)$ mass and with of 3637.7 ± 1.3 MeV/ c^2 and 10.4 ± 4.2 MeV, respectively.

For the P -wave singlet state, $h_c(1P)$, its first evidence

* E-mail: jiqingping@htu.edu.cn

† E-mail: fangss@ihep.ac.cn

‡ E-mail: wangzy@ihep.ac.cn

was reported by the Fermilab E760 experiment [11] and was based on the process of $p\bar{p} \rightarrow \pi^0 J/\psi$. This result was subsequently excluded by the E835 experiment with a larger data sample [12]. E835 Collaboration observed the $h_c(1P)$ signal via the process of $p\bar{p} \rightarrow h_c(1P) \rightarrow \gamma\eta_c(1S)$. Soon it was confirmed by the CLEO collaboration [13, 14], by studying the cascaded transition decay of $\psi(2S) \rightarrow \pi^0 h_c(1P)$ with $h_c(1P) \rightarrow \gamma\eta_c(1S)$. With this cascaded transition decay, the mass of $h_c(1P)$ was measured to be $(3525.28 \pm 0.19 \pm 0.12) \text{ MeV}/c^2$, and no measurement for its total decay width. In addition, the product BR was measured to be $(4.19 \pm 0.32 \pm 0.45) \times 10^{-4}$. They also presented an evidence for $h_c(1P)$ decays to multi-pion final states [15].

The discovery of $\eta_c(1S)$, $\eta_c(2S)$ and $h_c(1P)$ enriches highly the members of charmonium family. In the following decades the fruitful results on these states are reported at BESIII [16].

With runs in 2009 and 2012, the world's largest data samples of $1.31 \times 10^9 J/\psi$ events [17, 18] and $448.1 \times 10^6 \psi(2S)$ events [19, 20] are collected. The $\psi(2S)$ data sample is especially well suitable for studying charmonium transition decay to the lower-lying states, such as $\psi(2S) \rightarrow \gamma\eta_c(1S)$ and $\psi(2S) \rightarrow \pi^0 h_c(1P)$ with $h_c(1P) \rightarrow \gamma\eta_c(1S)$. The available $\eta_c(1S)$ and $h_c(1P)$ events via transition decays of $J/\psi(1S) \rightarrow \gamma\eta_c(1S)$, $\psi(2S) \rightarrow \gamma\eta_c(1S)$ and $\psi(2S) \rightarrow \pi^0 h_c(1P)$ are summarized in Table. I.

In this article, we first review theoretical underpinning in Sec. II discussing potential models and radia-

tive transitions, then review the progress on studying $\eta_c(1S)$, $\eta_c(2S)$ and $h_c(1P)$ decays at BESIII experiment in Sec. III, Sec. IV and Sec. V, respectively. Finally, we discuss the prospect in the future studies on these charmonium states at BESIII experiment in Sec. VI.

II. THEORETICAL UNDERPINNING

The lowest-lying and well-established charmonium states below the open-charm threshold can be used to precisely test predictions based on Quantum chromodynamics (QCD) and QCD-inspired models in a region where both perturbative (PQCD) and non-perturbative (NPQCD) aspect play a role. Determining the internal structure to previous established charmonium states, measuring masses and widths with high precision, precisely measuring transitions (both radiative and hadronic) between charmonium states and finding new decay modes can provide a unique and important perspective on the dynamics of strong force physics.

A. Potential model

1. Nonrelativistic potential model

Nonrelativistic (NR) potential model is a minimal model of the charmonium system, based on the wave functions determined by the Schrödinger equation with a conventional quarkonium potential. In NR potential model, the central potential is

$$V_0(r) = -\frac{4}{3} \frac{\alpha_s}{r} + br + \frac{32\pi\alpha_s}{9m_c^2} \tilde{\delta}_\sigma(r) \vec{S}_c \cdot \vec{S}_{\bar{c}} + \frac{1}{m_c^2} \left[\left(\frac{2\alpha_s}{r^3} - \frac{b}{2r} \right) \vec{L} \cdot \vec{S} + \frac{4\alpha_s}{r^3} T \right], \quad (1)$$

in which the spin-spin operator ($\vec{S} \cdot \vec{S}$) is for the mass splitting between spin-triplet and spin-singlet state, spin-orbit operator ($\vec{S} \cdot \vec{L}$) and tensor operator T are for the mass splitting between spin-triplet states [23]. Measurement the mass of charmonium state with high precision would be helpful to understanding the contribution from the spin associated.

2. Godfrey-Isgur relativized potential model

The Godfrey-Isgur (GI) model, which is a ‘‘relativized’’ extension of the nonrelativistic model, assumes a relativistic dispersion relation for the quark kinetic energy, a QCD-motivated running coupling $\alpha_s(r)$, a flavor-dependent potential smearing parameter σ , and replaces

factors of quark mass with quark kinetic energy. Details of the model and the method of solution may be found in Ref. [24].

According to the Refs. [23] [24], one important aspect about the two models is that the GI model gives reasonable accurate results for the spectrum and matrix elements of quarkonia of all u , d , s , c , b quark flavors, whereas the NR model is only fitted to the $c\bar{c}$ system.

B. Radiative Transitions

Transition ratio between charmonium states are calculated based on different potentials (nonrelativistic model or relativistic effect correction considered). Mass difference between charmonium spin-triplet and spin-singlet

TABLE I. The available $\eta_c(1S)$, $\eta_c(2S)$ and $h_c(1P)$ decays calculated with the 1.31×10^9 J/ψ events, 448.1×10^6 $\psi(2S)$ events and XYZ [21] data sample at BESIII. Here, we only list the h_c events at $\sqrt{S} = 4.23$ GeV.

| Decay mode | \mathcal{B} [3]/ σ [22] | $\eta_c(1S), \eta_c(2S)/h_c(1P)$ events |
|---|---|---|
| $J/\psi(1S) \rightarrow \gamma\eta_c(1S)$ | $(1.7 \pm 0.4) \times 10^{-2}$ | 2.2×10^7 |
| $\psi(2S) \rightarrow \gamma\eta_c(1S)$ | $(3.4 \pm 0.5) \times 10^{-3}$ | 1.5×10^6 |
| $\psi(2S) \rightarrow \gamma\eta_c(2S)$ | $(7.0 \pm 5.0) \times 10^{-4}$ | 3.1×10^5 |
| $\psi(2S) \rightarrow \pi^0 h_c(1P)$ | $(8.6 \pm 1.3) \times 10^{-4}$ | 3.9×10^5 |
| $e^+e^- \rightarrow \pi^+\pi^-h_c(1P)$ | $(50.2 \pm 2.7 \pm 4.6 \pm 7.9)\text{pb}$ | 2.3×10^4 |

state, as well as the transition ratio are also calculated with lattice QCD (LQCD) [25] [26]. Measurement the transition ratios could test the these predictions.

1. Electric dipole Transitions

The partial widths for electric dipole ($E1$) transitions is evaluated as [23]

$$\Gamma_{E1}(n^{2S+1}L_J \rightarrow n'^{2S'+1}L'_{J'} + \gamma) = \frac{4}{3}C_{fi}\delta_{SS'}e_c^2\frac{\alpha}{m_c^2}|\langle\psi_f|r|\psi_i\rangle|^2 \times E_\gamma^3\frac{E_f^{(c\bar{c})}}{M_i^{(c\bar{c})}}, \quad (2)$$

where $e_c = 2/3$ is the c -quark charge in units of $|e|$, α is the fine-structure constant, E_γ is the fine photon energy, $E_f^{(c\bar{c})}$ is the total energy of the final $c\bar{c}$ state, $M_i^{(c\bar{c})}$ is the mass of the initial $c\bar{c}$ state, the spatial matrix element $|\langle\psi_f|\psi_i\rangle|$ involves the initial and final radial wave functions, and the angular matrix element C_{fi} is

$$C_{fi} = \max(L, L')(2J' + 1)C_m^2, \quad (3)$$

with

$$C_m = \begin{Bmatrix} L' & J' & S \\ J & L & 1 \end{Bmatrix}$$

(See the previous $E1$ formula for definitions.)

Transitions from initial 1^{--} $c\bar{c}$ states are of greatest interest since these can be studied with high statistics at

e^+e^- machines, such as $\psi(2S) \rightarrow \gamma\chi_{c0,1,2}(1P)$, and the transitions from the $\psi(4040)$ and $\psi(4415)$

2. Magnetic dipole Transitions

Although Magnetic dipole transition ($M1$) rates are typically rather weaker than $E1$ rates, they are nonetheless interesting because they may allow access to spin-singlet states that are very difficult to produce otherwise. It is also interesting that the known $M1$ rates show serious disagreement between theory and experiment. This is in part due to the fact that $M1$ transitions between different spatial multiplets, such as $\psi(2S) \rightarrow \gamma\eta_c(1S)$, $J/\psi(1S) \rightarrow \gamma\eta_c(1S)$ and $\psi(2S) \rightarrow \gamma\eta_c(2S)$, are nonzero only due to small relative corrections to a vanishing lowest-order $M1$ matrix element.

The $M1$ radiative partial widths are evaluated using [23]

$$\Gamma_{M1}(n^{2S+1}L_J \rightarrow n'^{2S'+1}L'_{J'} + \gamma) = \frac{4}{3}\frac{2J'+1}{2L+1}\delta_{LL'}\delta_{S,S'\pm 1}e_c^2\frac{\alpha}{m_c^2}|\langle\psi_f|\psi_i\rangle|^2 \times E_\gamma^3\frac{E_f^{(c\bar{c})}}{M_i^{(c\bar{c})}}, \quad (4)$$

In Ref. [23], the $E1$ rates, as well as the $M1$ rates are

evaluated in both the NR potential model and the GI

model described in Ref. [24]. Better experimental data will be very important for improving our description of these apparently simple but evidently poorly understood $M1$ radiative transitions.

III. $\eta_c(1S)$ PHYSICS

A. $\eta_c(1S)$ resonance parameters

Although $\eta_c(1S)$ has been known for about thirty years [2], its resonant parameters are still have large uncertainties when compared to those of other charmonium states [3]. Early measurements about the $\eta_c(1S)$ properties using $J/\psi(1S)$ radiative transition [27, 28] found its mass and width to be about 2980 MeV/ c^2 and 10 MeV, respectively. However, the experiments including photon-photon fusion and B decays have appeared a significantly discrepancies on both mass and width [29–32]. In 2009, CLEO Collaboration pointed out a distortion of the $\eta_c(1S)$ line shape in $\psi(2S)$ decays using the $M1$ transition both $J/\psi(1S) \rightarrow \gamma\eta_c(1S)$ and $\psi(2S) \rightarrow \gamma\eta_c(1S)$ [33]. They attributed this distortion to the energy dependence of the $M1$ transition matrix element. The $h_c(1P) \rightarrow \gamma\eta_c(1S)$ transition can provide a new laboratory to study $\eta_c(1S)$ properties since the $\eta_c(1S)$ line shape in this transition should be generally normal due to the small non-resonant interfering backgrounds.

Better measurements of its mass and total width are still inspired. These measurements are performed via $M1$ transition ($\psi(2S) \rightarrow \gamma\eta_c(1S)$ [34] and $J/\psi(1S) \rightarrow \gamma\eta_c(1S)$ [35]) and $E1$ transition decay, $h_c(1P) \rightarrow \gamma\eta_c(1P)$ via $\psi(2S) \rightarrow \pi^0 h_c(1P)$ [36] involving $\eta_c(1S)$ at BESIII.

In the $M1$ transition decay $\psi(2S) \rightarrow \gamma\eta_c(1S)$ [34], six hadronic decay modes ($K_S K^+ \pi^-$, $K^+ K^- \pi^0$, $\eta \pi^+ \pi^-$, $K_S K^+ \pi^+ \pi^- \pi^-$, $K^+ K^- \pi^+ \pi^- \pi^0$, and $3(\pi^+ \pi^-)$ (where the inclusion of charge conjugate mode is implied) are adopted to reconstruct $\eta_c(1S)$ meson, and about 7000 events of $\eta_c(1S)$ signal are observed. The significant asymmetry (long tail in the low mass region while drop quickly in the high mass region) in the η_c line shape is seen, as shown in Fig. 2. The $\eta_c(1S)$ line shapes are described successfully using a combination of the energy-dependent hindered- $M1$ transition matrix element and a full interference with non-resonance $\psi(2S)$ radiative decays. The $\eta_c(1S)$ mass and width are measured to be $(2984.3 \pm 0.6 \pm 0.6)$ MeV/ c^2 and $(32.0 \pm 1.2 \pm 1.0)$ MeV by introducing the assumption of all radiative non-resonance events interference with the $\eta_c(1S)$. It is found that the significance of the interference is of order 15σ which affects the $\eta_c(1S)$ mass and width significantly, and may also have impacted all of the previous measurements on mass and width based on radiative transitions. The consistency between our experiment and

photon-photon fusion and B decays can partly clarify the discrepancy puzzle discussed above. As a parameter input of potential model as introduced in Sec. II A, the measurement precision of $\eta_c(1S)$ and $\eta_c(2S)$ resonant parameters has an obvious influence on the theoretical prediction. According to the measured results at BESIII, the hyperfine mass splitting is determined to be $\Delta M_{\text{hf}}(1S) \equiv M(J/\psi(1S)) - M(\eta_c(1S)) = 112.6 \pm 0.8$ MeV/ c^2 , which agrees well with recent lattice computations [37–39] as well as quark-model predictions [40], and sheds light on spin-dependent interactions in quarkonium states.

In the $M1$ transition decay $J/\psi(1S) \rightarrow \gamma\eta_c(1S)$ [35], $\eta_c(1S)$ is reconstructed with vector meson pair $\omega\omega$. The mass, width, and yield of the $\eta_c(1S)$ signal are determined by means of a partial wave analysis (PWA) after considering the interference effects with other contributions between $\eta_c(1S)$ and non- $\eta_c(1S)$ decay. The final $\omega\omega$ mass spectra and the fit results are shown in Fig. 3 (a), and the fit yields 1705 ± 58 events of $\eta_c(1S)$ signal observed. The $\eta_c(1S)$ mass and width using the radiative transition $J/\psi(1S) \rightarrow \gamma\eta_c(1S)$ is determined to be $(2985.9 \pm 0.7 \pm 2.1)$ MeV/ c^2 and $(33.8 \pm 1.6 \pm 4.1)$ MeV, respectively, which are in good agreement with the world average values, and also agree with the those obtained via studying $\psi(2S) \rightarrow \gamma\eta_c(1S)$ [34].

In the $E1$ transition decay $h_c(1P) \rightarrow \gamma\eta_c(1S)$ via $\psi(2S) \rightarrow \pi^0 h_c(1P)$ [36], $\eta_c(1S)$ is reconstructed with 16 $\eta_c(1S)$ exclusive hadronic final states. They are $p\bar{p}$, $2(\pi^+ \pi^-)$, $2(K^+ K^-)$, $K^+ K^- \pi^+ \pi^-$, $p\bar{p} \pi^+ \pi^-$, $3(\pi^+ \pi^-)$, $K^+ K^- 2(\pi^+ \pi^-)$, $K^+ K^- \pi^0$, $p\bar{p} \pi^0$, $K_S^0 K^\pm \pi^\mp$, $K_S^0 K^\pm \pi^\mp \pi^\pm \pi^\mp$, $\pi^+ \pi^- \eta$, $K^+ K^- \eta$, $2(\pi^+ \pi^-) \eta$, $\pi^+ \pi^- \pi^0 \pi^0$, and $2(\pi^+ \pi^- \pi^0)$. The $\eta_c(1S)$ line shape observed in this decay is not as asymmetric obviously as that observed in the $E1$ transition decay ($\psi(2S) \rightarrow \gamma\eta_c(1S)$ and $J/\psi(1S) \rightarrow \gamma\eta_c(1S)$). This phenomenon is introduced by the quite large decay ratio of $h_c(1P) \rightarrow \gamma\eta_c(1S)$, which is larger than 50% [3], resulting a small amplitude predicted for $h_c(1P)$ decaying to pseudoscalar meson via radiative decay and a negligible interference effects with $h_c(1S) \rightarrow \gamma\eta_c(1S)$. The $\eta_c(1S)$ resonance parameters are obtained by simultaneously fitting the $\eta_c(1S)$ mass spectrum for all 16 channels, as shown in Fig. 4, and about 831.9 ± 35.0 events of η_c signal are observed. The $\eta_c(1S)$ mass and width are $M(\eta_c(1S)) = (2984.49 \pm 1.16 \pm 0.52)$ MeV/ c^2 and $\Gamma(\eta_c(1S)) = (36.4 \pm 3.2 \pm 1.7)$ MeV, respectively, which are consistent with those via study the $\psi(2S)$ radiative decay $\psi(2S) \rightarrow \gamma\eta_c(1S)$ [34] and B -factory results from $\gamma\gamma \rightarrow \eta_c(1S)$ and B decays [41, 42]. This consistence indicates that there is large interference amplitude in the $E1$ transitions of $\psi(2S) \rightarrow \gamma\eta_c(1S)$ and $J/\psi(1S) \rightarrow \gamma\eta_c(1S)$, and it is reasonable to take it into account when measuring the resonance parameters of $\eta_c(1S)$ within these decays.

With weighted least squares method [43], and combining statistical and systematic errors in quadrature, the

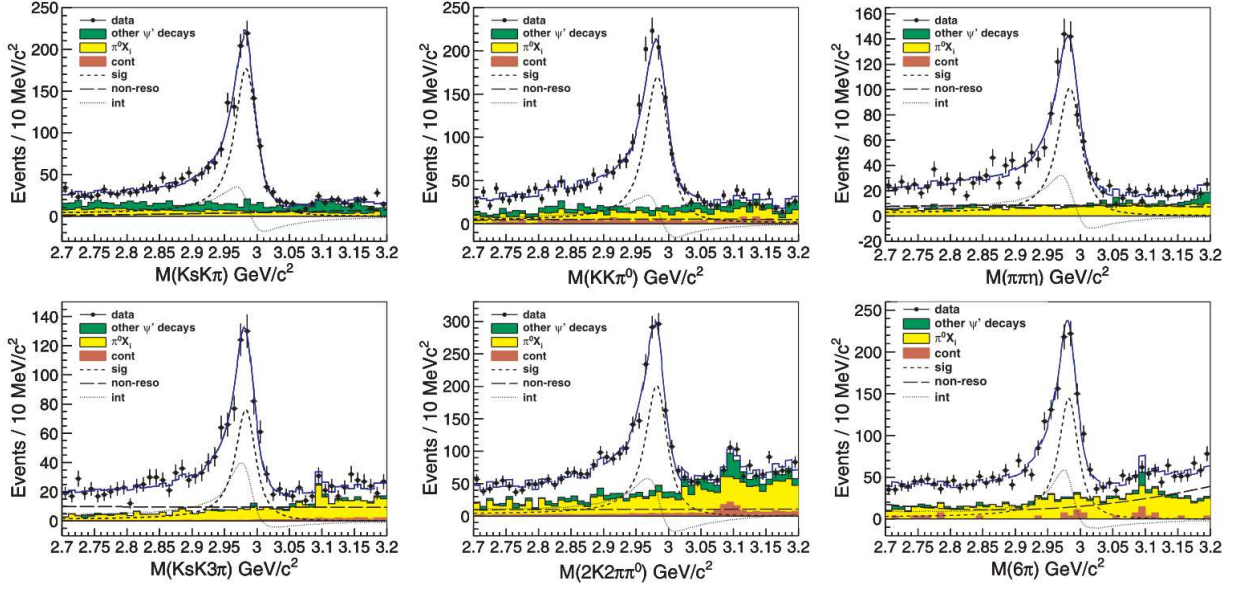


FIG. 2. Measurement of the mass and width of $\eta_c(1S)$ using $\psi(2S) \rightarrow \gamma\eta_c(1S)$. The invariant mass distributions for the decays $K_S K^+ \pi^-$, $K^+ K^- \pi^0$, $\eta \pi^+ \pi^-$, $K_S K^+ \pi^+ \pi^- \pi^-$, $K^+ K^- \pi^+ \pi^- \pi^0$, and $3(\pi^+ \pi^-)$, respectively, with the fit results (for the constructive solution) superimposed [34]. Dots with error bars are data, and the curves are total fit and each component. Charge conjugate modes are included.

averaged mass for $\eta_c(1S)$ at BESIII is (2984.68 ± 0.93) MeV/c^2 , and the mass splitting with S wave iso-spin triplet is $\Delta M_{\text{hf}}(1S) = (112.22 \pm 0.93)$ MeV/c^2 which agrees well with recent lattice computations [37–39] as well as quark-model predictions [40], and sheds light on spin-dependent interactions in quarkonium states.

B. $\eta_c(1S)$ decays

1. Decays into vector meson pairs

The processes $\eta_c(1S)$ decaying into vector meson (abbreviated as V hereafter) pairs are highly suppressed by the helicity selection rule (HSR) [44], but experiment gives extremely large results [45], in which the BRs of $\eta_c(1S) \rightarrow VV$ are measured to be $\mathcal{B}(\eta_c(1S) \rightarrow \rho\rho) = (1.23 \pm 0.37 \pm 0.50) \times 10^{-2}$, $\mathcal{B}(\eta_c(1S) \rightarrow K^* \bar{K}^*) = (10.3 \pm 2.6 \pm 4.3) \times 10^{-3}$, $\mathcal{B}(\eta_c(1S) \rightarrow \phi\phi) = (2.5 \pm 0.5 \pm 0.9) \times 10^{-3}$, $\mathcal{B}(\eta_c(1S) \rightarrow \omega\omega) < 6.3 \times 10^{-3}$ (90% C.L.), and $\mathcal{B}(\eta_c(1S) \rightarrow \omega\phi) < (1.7 \times 10^{-3})$ (90% C.L.), respectively. This large discrepancy between theoretical predictions and experimental measurements stands as a long-term puzzle existing in the charmonium physics. The higher order radiative corrections fail to solve this issue, since they are all suppressed by the light quark masses. Although beyond the scope of pQCD some non-perturbative models have been put forward and considered to be solutions to the problem, such as the intermediate meson exchange model [46], the charmonium light Fock component admixture model [47], the 3P_0 quark

pair creation mechanism [48], and long-distance intermediate meson loop effects [49].

Predictions based on next-to-leading order (NLO) PQCD calculations and the so-called higher-twist contributions are also performed [50–52]. The latter contribution is found to be dominate and give out a reasonably large decay width ($\sim 10^{-4}$), though it still deviates a lot from the experimental measurement ($\sim 10^{-3}$). To help understand the $\eta_c(1S)$ decay mechanism, high precision measurements of these BRs are desirable.

$\eta_c(1S) \rightarrow \omega\omega$, $\omega\phi$ and $\phi\phi$ are investigated via $J/\psi(1S) \rightarrow \gamma\eta_c(1S)$ at BESIII [35] [53]. Clear signal of $\eta_c(1S) \rightarrow \omega\omega$ are observed for the first time. As shown in Fig. 3 (a), by means of a partial wave analysis, the corresponding BF is measured to be $\mathcal{B}(\eta_c(1S) \rightarrow \omega\omega) = (2.88 \pm 0.10 \pm 0.46 \pm 0.68) \times 10^{-3}$, where the external uncertainty refers to that arising from the BF of the decay $J/\psi \rightarrow \gamma\eta_c(1S)$. Fig. 3 (b) and (c) show the invariant masses of $\phi\phi$ and $\omega\phi$. BR of $\eta_c(1S) \rightarrow \phi\phi$, $(2.5 \pm 0.3^{+0.3}_{-0.7} \pm 0.6) \times 10^{-3}$, is consistent with the previous measurements [45], but the precision is improved. No significant signal for $\eta_c(1S) \rightarrow \omega\phi$ is observed. The upper limit at 90% C.L. on the BR is determined to be $\mathcal{B}(\eta_c(1S) \rightarrow \omega\phi) < 2.5 \times 10^{-4}$, which is one order magnitude more stringent than the previous upper limit [45].

To understand the HSR violation mechanism, a comparison between the experimental measurements and the theoretical predictions based on the light quark mass correction [48], the 3P_0 quark pair creation mechanism [50] and the intermediate meson loop effects [49] is presented in Table II. We can find that the measured $\mathcal{B}(\eta_c(1S) \rightarrow$

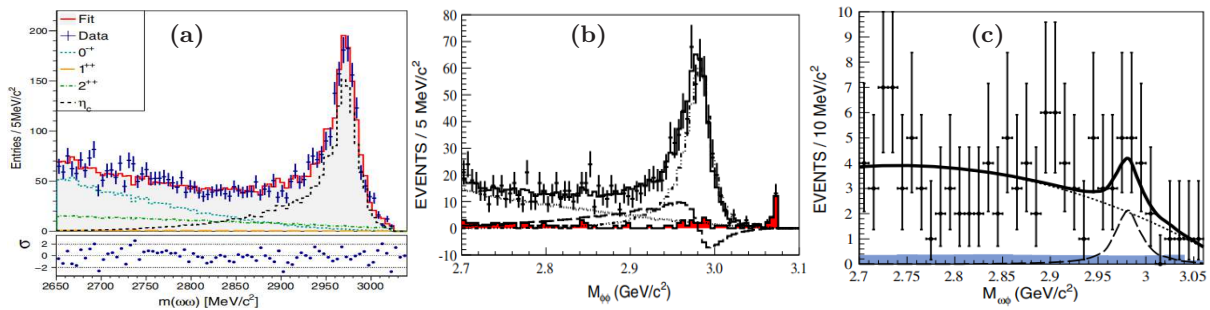


FIG. 3. Observation of $\eta_c(1S) \rightarrow \omega\omega$ [35], and improved measurements of BFs for $\eta_c(1S) \rightarrow \phi\phi$ and $\omega\phi$ [53]. Projection of the best fit results onto the $\omega\omega$ (a), $\phi\phi$ (b) and $\omega\phi$ (c) mass.

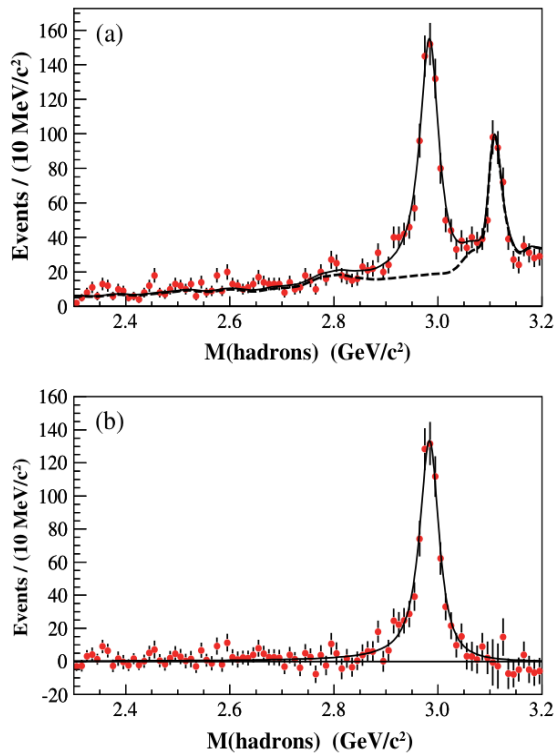


FIG. 4. The hadronic mass spectrum in $\psi(2S) \rightarrow \pi^0 h_c(1P)$, $h_c(1P) \rightarrow \gamma \eta_c(1S)$, $\eta_c(1S) \rightarrow X_i$ summed over the 16 final state X_i . The dots with error bars represent the hadronic mass spectrum in data [36]. The solid line shows the total fit function and the dashed line is the background component of the fit. (b) The background-subtracted hadronic mass spectrum with the signal shape overlaid.

$\omega\omega$) and $\mathcal{B}(\eta_c(1S) \rightarrow \phi\phi)$ are close to the predictions of the 3P_0 quark model [50] and the meson loop effects [49]. In addition, the measured upper limit for $\mathcal{B}(\eta_c(1S) \rightarrow \omega\phi)$ is comparable with the predicted one in [49]. The consistency between data and the theoretical calculation indicates the importance of QCD higher twist contributions or the presence of a NPQCD mechanism.

2. Decays into baryon pairs

$\eta_c(1S)$ decaying to baryon-anti-baryon pairs are also supposed to be highly suppressed by the HSR as a consequence of the PQCD framework. The contradictions between PQCD calculations and experimental measurements also exist in this process, as is the discrepancy for $\eta_c(1S) \rightarrow VV$. Many theoretical models have been developed to understand these contradictions, such as by the quark-diquark model for the proton [55, 56], constituent quark-mass corrections [57, 58], mixing between the charmonium state and the glueball [59], and the quark pair creation model [60]. However, none of them is perfect enough.

In Refs. [61, 62], a theory related to intermediate meson loop (IML) transitions is proposed, where the long-distance interaction can evade the OZI rule and allow the violation of the PQCD HSR. Further calculations on the BFs of $\eta_c(1S) \rightarrow B_8 \bar{B}_8$, $\chi_{c0}(1P) \rightarrow B_8 \bar{B}_8$ and $h_c(1P) \rightarrow B_8 \bar{B}_8$, where B_8 denote the octet baryon, based on charmed-meson loops were carried out [63], and the results agree with the measured BFs of $\eta_c(1S) \rightarrow p\bar{p}$ and $\eta_c(1S) \rightarrow \Lambda\bar{\Lambda}$, but with large uncertainty [64] [65].

BESIII Collaboration reported a series of results on $\eta_c(1S) \rightarrow B_8 \bar{B}_8$ via $J/\psi(1S)$ radiative transition $J/\psi(1S) \rightarrow \gamma \eta_c(1S)$ for the first time. e.g., $\eta_c(1S) \rightarrow \Lambda\bar{\Lambda}$, $\Sigma^+\bar{\Sigma}^-$ and $\Xi^-\bar{\Xi}^+$ [65] [66], as well as the decay $\eta_c(1S) \rightarrow p\bar{p}$ via $\psi(2S) \rightarrow \pi^0 h_c(1P)$ [36] and $e^+e^- \rightarrow \pi^+\pi^- h_c(1P)$ [67], respectively (see detail for $\eta_c(1S) \rightarrow p\bar{p}$ in Sec. III B 3). Figure 5 (a), (b) and (c) show the invariant mass spectrum for $\Lambda\bar{\Lambda}$, $\Sigma^+\bar{\Sigma}^-$ and $\Xi^-\bar{\Xi}^+$ final states, respectively. The corresponding measured BRs are listed in Tab. III. The decay $\eta_c(1S) \rightarrow \Sigma^+\bar{\Sigma}^-$ and $\Xi^-\bar{\Xi}^+$ are observed for the first time, and BR for $\eta_c(1S) \rightarrow p\bar{p}$ agrees with the previous measurements, but with higher precision [64].

Table. III compares the results of BESIII measurement of BRs for $\eta_c(1S) \rightarrow B_8 \bar{B}_8$ with the previous results and theoretical predictions by the intermediate charmed hadron loop transitions [63]. The measured BF of $\eta_c(1S) \rightarrow \Sigma^+\bar{\Sigma}^-$ is larger than the predictions from charmed-meson loop calculations [63], while the mea-

TABLE II. Comparison of BESIII measurement of BRs for $\eta_c(1S) \rightarrow \omega\omega, \phi\phi$ and $\omega\phi$ with the previous results and theoretical predictions, where ‘-’ denotes there is no prediction.

| | | $\mathcal{B}(\eta_c(1S) \rightarrow \omega\omega)(\times 10^{-3})$ | $\mathcal{B}(\eta_c(1S) \rightarrow \phi\phi)(\times 10^{-3})$ | $\mathcal{B}(\eta_c(1S) \rightarrow \omega\phi)(\times 10^{-3})$ |
|------------------|--------------------------|--|--|--|
| Exp. results | BESIII [35] [53] | $2.88 \pm 0.10 \pm 0.46 \pm 0.68$ | $2.5 \pm 0.3^{+0.3}_{-0.7} \pm 0.6$ | < 0.25 |
| | BESII [45] | $< 6.3 \times 10^{-3}$ | 1.9 ± 0.6 | < 1.7 |
| The. predictions | PQCD [48] | 0.09~0.13 | 0.7~0.8 | — |
| | 3P_0 quark model [50] | 1.5~1.6 | 1.9~2.0 | 0 |
| | Charm meson loop [49] | 1.8 | 2.0 | < 0.33 |

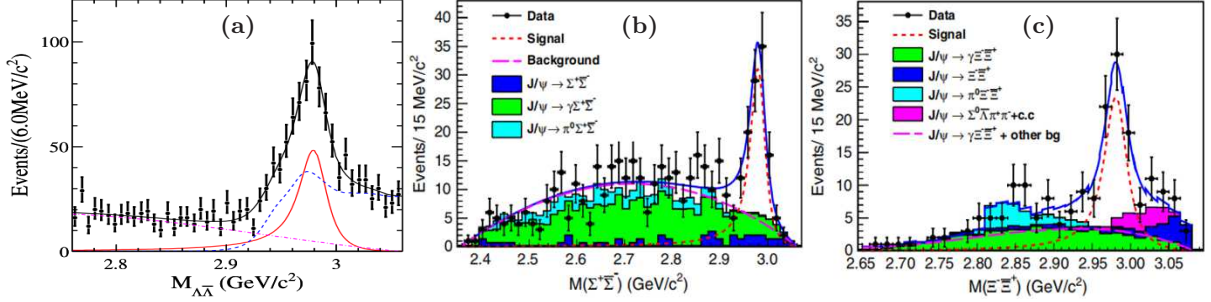


FIG. 5. Observation of $\eta_c(1S) \rightarrow \Lambda\bar{\Lambda}$ [65], $\Sigma^+\bar{\Sigma}^-$ and $\Xi^-\bar{\Xi}^+$ [66]. Invariant-mass distributions of $\Lambda\bar{\Lambda}$ (a), $\Sigma^+\bar{\Sigma}^-$ (b), and $\Xi^-\bar{\Xi}^+$ (c), as well as the fitted curves. Dots with error bars are data, and the histograms are the backgrounds from simulated J/ψ decays. Solid lines are the total fit results, signals are shown in short-dashed lines, and backgrounds are shown as long-dashed lines and shaded histograms.

sured BF of $\eta_c(1S) \rightarrow \Xi^-\bar{\Xi}^+$ agrees with the prediction. Among the four $\eta_c(1S)$ baryonic decays ($\eta_c(1S) \rightarrow p\bar{p}$, $\Lambda\bar{\Lambda}$, $\Sigma^+\bar{\Sigma}^-$, and $\Xi^-\bar{\Xi}^+$), only $\eta_c(1S) \rightarrow \Sigma^+\bar{\Sigma}^-$ disagrees with the prediction, which may indicate the violation of SU(3) symmetry.

3. Decay into light hadrons

As mentioned before, the $\eta_c(1S)$ decays to light hadron final states has been investigated with $h_c(1P) \rightarrow \gamma\eta_c(1S)$ via $\psi(2S) \rightarrow \pi^0 h_c(1P)$. In addition, BESIII detector has also collected sizable data samples between 4.009 and 4.600 GeV (called ‘XYZ data’ hereafter) since 2013 to study the XYZ states [68]. A large production rate of $e^+e^- \rightarrow \pi^+\pi^-h_c(1P)$ has been found [22]. The total number of $h_c(1P)$ events in all these data samples combined is comparable to that from $\psi(2S) \rightarrow \pi^0 h_c(1P)$ according to the measured cross section and the corresponding integrated luminosity at each energy point. The $h_c(1P)$ is tagged by the recoil mass (RM) of $\pi^+\pi^-$ in XYZ data. Compared with that tagged by $RM(\pi^0)$ in $\psi(2S)$ data sample, the former has lower background and higher detection efficiency than the latter due to the better momentum resolution for charged track. Using the data at $\sqrt{s} = 4.23, 4.26, 4.36$ and 4.42 GeV, the BF

of four η_c exclusive decays are measured via the process $e^+e^- \rightarrow \pi^+\pi^-h_c(1P)$, $h_c(1P) \rightarrow \gamma\eta_c(1S)$ [67]. These exclusive decays are $\eta_c(1S) \rightarrow K^+K^-\pi^0$, $K_S^0 K^\pm \pi^\mp$, $2(\pi^+\pi^-\pi^0)$ and $p\bar{p}$, respectively. The BFs of $\eta_c(1S)$ exclusive decays are obtained by a simultaneous fit to the $RM(\pi^+\pi^-\gamma)$ for both inclusive and exclusive modes. As a result, we obtained the highest precision compared to the previous single measurement. The measured BFs are summarized in Tab. IV. A few more discussion can be found in Sec. VB 2.

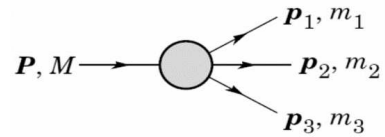


FIG. 6. Feynman diagram of the three-body decay.

The decay width of $\eta_c(1S)$ into a pseudoscalar glueball is computed in the framework of a $U(4)_r \times U(4)_l$ symmetric linear sigma model with (pseudo-)scalar and (axial-) vector mesons [69]. Using the notation of Fig. 6 and the definition $m_{ij} = m_i + m_j$, the corresponding expression for the three-body decay width of the process $A \rightarrow B_1 B_2 B_3$ reads [3]:

TABLE III. Comparison of BESIII measurement of BRs for $\eta_c(1S) \rightarrow B_s \bar{B}_s$ with the previous results and theoretical predictions by the intermediate charmed hadron loop transitions [63]. Here, the third uncertainty is from input branching fractions taken from Ref. [3].

| | $\mathcal{B}(\eta_c(1S) \rightarrow p\bar{p})(\times 10^{-4})$ | $\mathcal{B}(\eta_c(1S) \rightarrow \Lambda\bar{\Lambda})(\times 10^{-4})$ | $\mathcal{B}(\eta_c(1S) \rightarrow \Sigma^-\bar{\Sigma}^+)(\times 10^{-4})$ | $\mathcal{B}(\eta_c(1S) \rightarrow \Xi^-\bar{\Xi}^+)(\times 10^{-4})$ |
|-----------------------------------|--|---|--|--|
| Exp. results | $12.0 \pm 2.6 \pm 1.5$ [67] $15.8 \pm 1.2^{+1.8}_{-2.2} \pm 4.7$ [64] | $11.6 \pm 1.2 \pm 1.9 \pm 2.8$ [65] $8.7^{+2.4+0.9}_{-2.1-1.4} \pm 2.7$ [64] | $21.1 \pm 2.8 \pm 1.8 \pm 5.0$ [66] | $8.9 \pm 1.6 \pm 0.8 \pm 2.1$ [66] |
| The. predictions (Hadron loop) | 9.0 ~ 17.0 | 6.3 ~ 12.5 | 5.05 ~ 10.0 | 4.82 ~ 9.56 |

TABLE IV. Review of the measured BF of $\eta_c(1S) \rightarrow X_i$ at BESIII. $\mathcal{B}_{\psi(2S)}$ denote the BFs measured with $\psi(2S) \rightarrow \pi^0 h_c(1P)$ and $h_c(1P) \rightarrow \gamma \eta_c(1S)$, $\mathcal{B}_{e^+e^-}$ denote the BFs measured with $e^+e^- \rightarrow \pi^+\pi^- h_c(1P)$ and $h_c(1P) \rightarrow \gamma \eta_c(1S)$. Here, X_i denotes hadronic final states. For the measured BFs, the first uncertainties are statistical, second ones are systematic, third ones are uncertainties due to $\mathcal{B}(\psi(2S) \rightarrow \pi^0 h_c(1P))$ and $\mathcal{B}(h_c(1P) \rightarrow \gamma \eta_c(1S))$. The last column gives the status of $\mathcal{B}_{\eta_c(1S) \rightarrow X_i}^{\text{PDG}}$ before the BESIII experiment.

| Decay mode | $\mathcal{B}_{\psi(2S)}(10^{-2})$ [36] | $\mathcal{B}_{e^+e^-}(10^{-2})$ [67] | Comment(10^{-2}) |
|--|--|--------------------------------------|----------------------|
| $\eta_c(1S) \rightarrow p\bar{p}$ | $0.15 \pm 0.04 \pm 0.02 \pm 0.01$ | $0.120 \pm 0.026 \pm 0.015$ | 0.141 ± 0.017 |
| $\eta_c(1S) \rightarrow 2(\pi^+\pi^-)$ | $1.72 \pm 0.19 \pm 0.25 \pm 0.17$ | ... | 0.86 ± 0.13 |
| $\eta_c(1S) \rightarrow K^+K^-K^+K^-$ | $0.22 \pm 0.08 \pm 0.03 \pm 0.02$ | ... | 0.134 ± 0.032 |
| $\eta_c(1S) \rightarrow K^+K^-\pi^+\pi^-$ | $0.95 \pm 0.17 \pm 0.13 \pm 0.09$ | ... | 0.61 ± 0.12 |
| $\eta_c(1S) \rightarrow p\bar{p}\pi^+\pi^-$ | $0.53 \pm 0.15 \pm 0.08 \pm 0.05$ | ... | < 1.2 (at 90% C.L.) |
| $\eta_c(1S) \rightarrow 3(\pi^+\pi^-)$ | $2.02 \pm 0.36 \pm 0.36 \pm 0.19$ | ... | 1.5 ± 0.5 |
| $\eta_c(1S) \rightarrow K^+K^-2(\pi^+\pi^-)$ | $0.83 \pm 0.39 \pm 0.15 \pm 0.08$ | ... | 0.71 ± 0.29 |
| $\eta_c(1S) \rightarrow K^+K^-\pi^0$ | $1.04 \pm 0.17 \pm 0.11 \pm 0.10$ | $1.15 \pm 0.12 \pm 0.10$ | 1.2 ± 0.1 |
| $\eta_c(1S) \rightarrow p\bar{p}\pi^0$ | $0.35 \pm 0.11 \pm 0.05 \pm 0.03$ | ... | first measurement |
| $\eta_c(1S) \rightarrow K_S^0 K^\pm \pi^\mp$ | $2.60 \pm 0.29 \pm 0.34 \pm 0.25$ | $2.60 \pm 0.21 \pm 0.20$ | 2.4 ± 0.2 |
| $\eta_c(1S) \rightarrow K_S^0 K^\pm \pi^\mp \pi^\pm \pi^\mp$ | $2.75 \pm 0.51 \pm 0.47 \pm 0.27$ | ... | first measurement |
| $\eta_c(1S) \rightarrow \pi^+\pi^-\eta$ | $1.66 \pm 0.34 \pm 0.26 \pm 0.16$ | ... | 4.9 ± 1.8 |
| $\eta_c(1S) \rightarrow K^+K^-\eta$ | $0.48 \pm 0.23 \pm 0.07 \pm 0.05$ | ... | < 1.5 (at 90% C.L.) |
| $\eta_c(1S) \rightarrow 2(\pi^+\pi^-)\eta$ | $4.40 \pm 0.86 \pm 0.85 \pm 0.42$ | ... | first measurement |
| $\eta_c(1S) \rightarrow \pi^+\pi^-\pi^0\pi^0$ | $4.66 \pm 0.50 \pm 0.76 \pm 0.45$ | ... | first measurement |
| $\eta_c(1S) \rightarrow 2(\pi^+\pi^-\pi^0)$ | $17.23 \pm 1.70 \pm 2.29 \pm 1.66$ | $15.3 \pm 1.8 \pm 1.8$ | first measurement |

$$\begin{aligned}
& \Gamma(A \rightarrow B_1 B_2 B_3) \\
&= \frac{S_{A \rightarrow B_1 B_2 B_3}}{32(2\pi)^3 M^3} \int_{(m_1+m_2)^2}^{(M-m_3)^2} | -i\mathcal{M}_{A \rightarrow B_1 B_2 B_3} |^2 \\
& \times \sqrt{\frac{(-m_1 + m_{12} - m_2)(m_1 + m_{12} - m_2)(-m_1 + m_{12} + m_2)(m_1 + m_{12} + m_2)}{m_{12}^2}} \\
& \times \sqrt{\frac{(-m_1 + m_{12} - m_3)(m_1 + m_{12} - m_3)(-m_1 + m_{12} + m_3)(m_1 + m_{12} + m_3)}{m_{12}^2}} dm_{12}^2,
\end{aligned} \tag{5}$$

where $\mathcal{M}_{A \rightarrow B_1 B_2 B_3}$ is the corresponding tree-level decay amplitude, and $S_{A \rightarrow B_1 B_2 B_3}$ is a symmetrization factor (equal to 1 if the B_i are all different, equal to 2 for two identical particles in the final state, and equal to 6 for three identical particles). Using the general formula for the three-body decay width for η_c Eq. 5, the corresponding tree-level decay amplitudes for $\eta_c(1S) \rightarrow \eta\eta\eta'$ are obtained and the corresponding partial decay widths of

$\eta_c(1S) \rightarrow \eta\eta\eta'$ are predicted to be $\Gamma(\eta_c(1S) \rightarrow \eta\eta\eta') = 0.045 \pm 0.014$ MeV. Experimentally, first observation of $\eta_c(1S) \rightarrow \eta\eta\eta'$ via $J/\psi(1S) \rightarrow \gamma\eta\eta\eta'$ is reported at BESIII [70]. Figure 7 shows the fit results for $\eta_c(1S)$ in the invariant mass distribution of $\eta\eta\eta'$ with $\eta' \rightarrow \gamma\pi^+\pi^-$ and $\eta' \rightarrow \eta\pi^+\pi^-$, respectively. A clear $\eta_c(1S)$ signal is seen, and the $\mathcal{B}(J/\psi(1S) \rightarrow \gamma\eta_c(1S)) \times \mathcal{B}(\eta_c(1S) \rightarrow \eta\eta\eta')$ is determined to be $(4.86 \pm 0.62 \pm 0.45) \times 10^{-5}$, which is

compatible with the theoretical prediction of partial decay width of $\eta_c(1S) \rightarrow \eta\eta'$ in Ref. [69].

4. Decays into $\gamma\gamma$

The quarkonium annihilation rates are used to evaluate the strong fine-structure constant α_S . The square of the wave function at the origin cancels out in the ratio of partial widths [71],

$$\frac{\Gamma(\eta_c(1S) \rightarrow \gamma\gamma)}{\Gamma(J/\psi(1S) \rightarrow \mu^+\mu^-)} = \frac{4}{3} \left[1 + 1.96 \frac{\alpha_S(m_c^2)}{\pi} \right], \quad (6)$$

Using the ‘evaluated’ partial widths in Ref. [3], $\Gamma(\eta_c(1S) \rightarrow \gamma\gamma) = 5.15 \pm 0.35$ keV and $\Gamma(J/\psi(1S) \rightarrow \mu^+\mu^-) = 5.54 \pm 0.17$ keV, one finds that $(3/4)\Gamma(\eta_c(1S) \rightarrow \gamma\gamma)/\Gamma(J/\psi(1S) \rightarrow \mu^+\mu^-) = 0.93 \pm 0.07$, which is consistent with Eq. 6 but not precise enough to test the QCD model. A more precise test would have taken into account $m(J/\psi(1S)) \neq 2m_c$ and the running of α_S .

The total width of $\eta_c(1S)$ is dominated by the gg final state. Its value is 32.0 ± 0.7 MeV [3]. By inputting the value of $\Gamma(\eta_c(1S) \rightarrow \gamma\gamma)$, one can determine the $gg/\gamma\gamma$ ratio to be

$$\frac{\Gamma(\eta_c(1S) \rightarrow gg)}{\Gamma(\eta_c(1S) \rightarrow \gamma\gamma)} = \frac{9[\alpha_S(m_c^2)]^2}{8\alpha^2} \left[1 + 8.2 \frac{\alpha_S(m_c^2)}{\pi} \right], \quad (7)$$

, which induces to $\alpha_S(m_c^2)$. This value should be regarded with caution in view of the large QCD correction factor $1 + 8.2\alpha_S/\pi \sim 1.8$.

Evidence of the $\eta_c(1S) \rightarrow \gamma\gamma$ decay is reported at BESIII [72], and the branching fraction of $J/\psi \rightarrow \gamma\eta_c(1S)$ and $\eta_c(1S) \rightarrow \gamma\gamma$ is determined to be $\mathcal{B}(J/\psi \rightarrow \gamma\eta_c(1S), \eta_c(1S) \rightarrow \gamma\gamma) = (4.5 \pm 1.2 \pm 0.6) \times 10^{-6}$, which agrees with the result from two-photon fusion [3].

5. Decay into CP and isospin violation modes

Search for the source of CP violation is one of the hottest topic at present. CP symmetry violation has important consequences; it is one of the key ingredients for the matter-antimatter asymmetry in our Universe. CP violation can be experimentally searched for in processes such as meson decays. The decays $\eta_c(1S) \rightarrow \pi^+\pi^-$ and $\pi^0\pi^0$, which violate both P and CP invariance, provide an excellent laboratory for testing the validity of symmetries of the physical world. In the SM, such decays can proceed only via the weak interaction with a BF of order 10^{-27} , according to Ref. [73]. Higher BFs are possible either by introducing a CP violating term in the QCD Lagrangian (a BR up to 10^{-17} can be obtained in this scheme) of allowing CP violation in the extended Higgs sector (with BF up to 10^{-15}), as described in

Ref. [73]. The detection of these decays at any level accessible today would be the signal P and CP violations from new sources, beyond any considered extension of the SM. The available results for $\eta_c(1S) \rightarrow \pi^+\pi^-$ and $\pi^0\pi^0$ are $\mathcal{B}(\eta_c(1S) \rightarrow \pi^+\pi^-) < 6 \times 10^{-4}$ and $\mathcal{B}(\eta_c(1S) \rightarrow \pi^0\pi^0) < 4 \times 10^{-4}$ at the 90% C.L. [74], respectively. Searching for these decays directly via $J/\psi(1S) \rightarrow \gamma\eta_c(1S)$ at BESIII based on the first round $J/\psi(1S)$ data sample are preformed [75]. The final $\pi^+\pi^-$ and $\pi^0\pi^0$ mass spectra, as well as the fit result are shown in Fig. 8. No significant $\eta_c(1S)$ signal is observed. Using the Bayesian method, the 90% C.L. upper limits are determined to be $\mathcal{B}(\eta_c(1S) \rightarrow \pi^+\pi^-) < 1.3 \times 10^{-4}$ and $\mathcal{B}(\eta_c(1S) \rightarrow \pi^0\pi^0) < 4.2 \times 10^{-5}$. These results provide experimental limits for theoretical models, and predict how much CP and P violation may be observed in $\eta_c(1S)$ meson decays.

Search for the isospin violating mode $\eta_c(1S) \rightarrow \pi^+\pi^-\pi^0$ is performed for the first time [76] at BESIII using two rounds $\psi(2S)$ data sample. The final $\pi^+\pi^-\pi^0$ mass spectra, as well as the fit result are shown in Figure 9. No obvious $\eta_c(1S)$ signal is seen, and the upper limit on $\mathcal{B}(\psi(2S) \rightarrow \gamma\eta_c(1S)) \times \mathcal{B}(\eta_c(1S) \rightarrow \pi^+\pi^-\pi^0)$ is 1.6×10^{-6} is given at 90% C.L.. Using the BF of $\psi(2S) \rightarrow \gamma\eta_c(1S)$, $[3.4 \pm 0.5] \times 10^{-3}$, the upper limit for $\mathcal{B}(\eta_c(1S) \rightarrow \pi^+\pi^-\pi^0)$ is calculated to be 5.5×10^{-4} . This is important to test isospin symmetry [77, 78].

IV. $\eta_c(2S)$ PHYSICS

The production of the $\eta_c(2S)$ through a radiative transition from the $\psi(2S)$ involves a charmed-quark spin-flip and, thus, proceeds via a M1 transition. The BF has been predicted in the range $\mathcal{B}(\psi(2S) \rightarrow \gamma\eta_c(2S)) = (0.1 - 6.2) \times 10^{-4}$ [79–81]. A phenomenological prediction, by assuming that the matrix element governed $\psi(2S) \rightarrow \gamma\eta_c(2S)$ is the same as that for $J/\psi \rightarrow \gamma\eta_c(1S)$, is given by

$$\mathcal{B}(\psi(2S) \rightarrow \gamma\eta_c(2S)) = \frac{k_{\psi(2S)}^3}{k_{J/\psi}^3} \frac{\Gamma_{J/\psi}}{\Gamma_{\psi(2S)}} \mathcal{B}(J/\psi \rightarrow \gamma\eta_c(1S)) \quad (8)$$

where $k_{\psi(2S)}$ ($k_{J/\psi}$) is the photon energy for the $\psi(2S) \rightarrow \gamma\eta_c(2S)$ ($J/\psi \rightarrow \gamma\eta_c(1S)$) transition, $\Gamma_{\psi(2S)}$ ($\Gamma_{J/\psi}$) is the $\psi(2S)$ (J/ψ) full width, and $\mathcal{B}(J/\psi \rightarrow \gamma\eta_c) = (1.7 \pm 0.4)\%$ [3]. Using the PDG values for $k_{\psi(2S)}$, $k_{J/\psi}$, $\Gamma_{\psi(2S)}$ and $\Gamma_{J/\psi}$ leads to a prediction of $\psi(2S) \rightarrow \gamma\eta_c(2S) = (3.9 \pm 1.1) \times 10^{-4}$ [82].

Early, this transition decay $\psi(2S) \rightarrow \gamma\eta_c(2S)$ has been searched for by Crystal Ball [83], BES [84, 85], and CLEO [82]. No convincing signal was observed by any of these experiments.

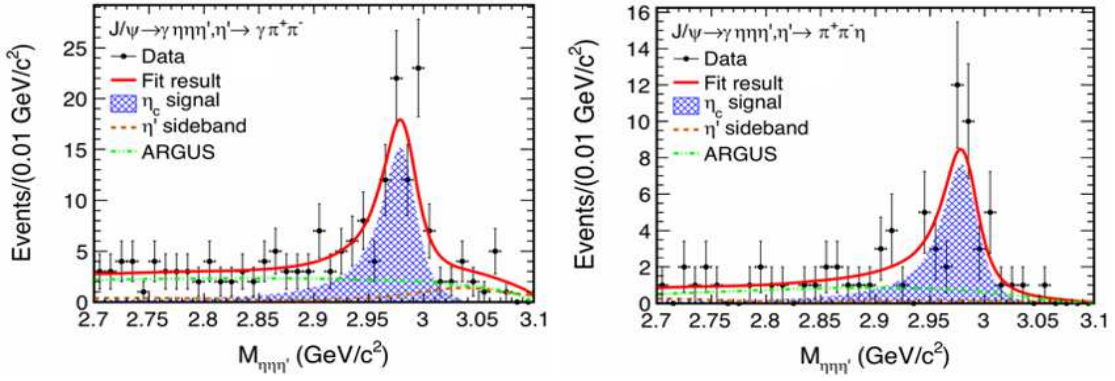


FIG. 7. Fit results for $\eta_c(1S)$ in the invariant mass distribution of $\eta\eta'$ for the decays of $\eta' \rightarrow \gamma\pi^+\pi^-$ and $\eta' \rightarrow \eta\pi^+\pi^-$, respectively. [70].

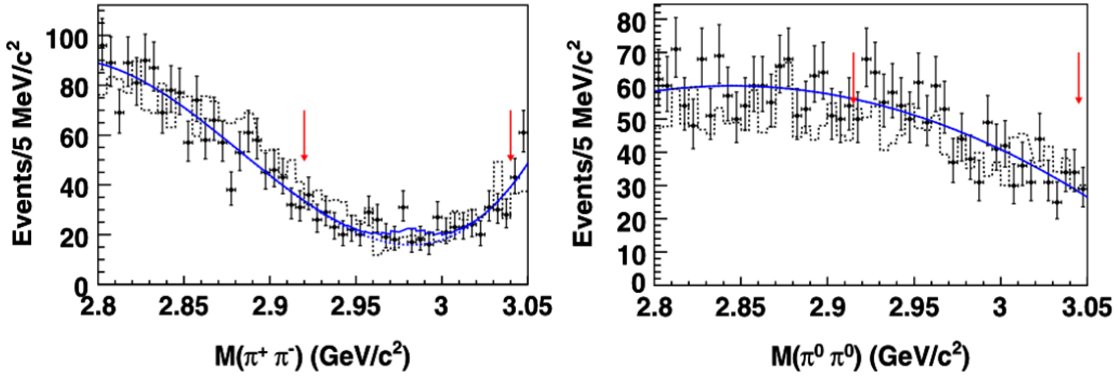


FIG. 8. Search for CP and P violating pseudoscalar decays into $\pi\pi$. The $\pi^+\pi^-$ and $\pi^0\pi^0$ invariant mass distributions of the final candidate events in the $\eta_c(1S)$ mass region. The dots with error bars are data, the solid lines are the best fit, and the dashed histograms are the sum of all the simulated normalized backgrounds. The arrows show mass regions which contain around 95% of the signal according to MC simulations [75].

A. First observation of $\eta_c(2S)$ signal in $\psi(2S)$ M1 transition

Compared with $E1$ transitions, the rates for $M1$ transitions between charmonium states are much lower. With the first round $\psi(2S)$ events, the $M1$ transition between the radial excited charmonium S -wave spin-triplet and the spin-singlet states: $\psi(2S) \rightarrow \gamma\eta_c(2S)$ was observed for the first time with $\eta_c(2S) \rightarrow K_S^0 K^\pm \pi^\mp$ and $K^+ K^- \pi^0$ modes. The final $K_S^0 K^\pm \pi^\mp$ and $K^+ K^- \pi^0$ mass spectra and the fit results are shown in Fig. 10 (a) and (b), respectively. The fit yields for the $\eta_c(2S)$ signal events are 81 ± 14 for the $K_S^0 K^\pm \pi^\mp$ mode and 46 ± 11 for the $K^+ K^- \pi^0$ mode; the overall statistical significance of the signal is larger than 10σ [86].

The mass of the $\eta_c(2S)$ is measured to be $(3637.6 \pm 2.9 \pm 1.6)$ MeV/ c^2 , the width $(16.9 \pm 6.4 \pm 4.8)$ MeV, in good agreement with the PDG values [3], and the product BF $\mathcal{B}(\psi(2S) \rightarrow \gamma\eta_c(2S)) \times \mathcal{B}(\eta_c(2S) \rightarrow K\bar{K}\pi) = (1.30 \pm 0.20 \pm 0.30) \times 10^{-5}$. Combining this result with a BABAR measurement of $\mathcal{B}(\eta_c(2S) \rightarrow K\bar{K}\pi)$ [87], the $M1$ transition rate is determined to be $\mathcal{B}(\psi(2S) \rightarrow$

$\gamma\eta_c(2S)) = (6.8 \pm 1.1 \pm 4.5) \times 10^{-4}$. This agrees with theoretical calculations [79–81] and naive estimates based on the $J/\psi(1S) \rightarrow \gamma\eta_c(1S)$ transition [82].

B. Evidence for $\eta_c(2S)$ in $\psi(2S) \rightarrow \gamma K_S^0 K^\pm \pi^\mp \pi^+ \pi^-$

Using the same sample as mentioned above, search for the $M1$ radiative transition $\psi(2S) \rightarrow \gamma\eta_c(2S)$ by reconstructing the exclusive $\eta_c(2S) \rightarrow K_S^0 K^\pm \pi^\mp \pi^+ \pi^-$ decay is performed [88]. The final $\eta_c(2S) \rightarrow K_S^0 K^\pm \pi^\mp \pi^+ \pi^-$ mass spectra and the fit results are shown in Fig. 10 (c). The result for the yield of $\eta_c(2S)$ events is 57 ± 17 with a significance of 4.2σ . The measured mass of the $\eta_c(2S)$ is $(3646.9 \pm 1.6 \pm 3.6)$ MeV/ c^2 , and the width is $(9.9 \pm 4.8 \pm 2.9)$ MeV. Comparing with BESIII previous measurement [86], the width is consistent with each other within one standard deviation and the mass is about two standard deviations. The BF is measured to be $\mathcal{B}(\psi(2S) \rightarrow \gamma\eta_c(2S)) \times \mathcal{B}(\eta_c(2S) \rightarrow K_S^0 K^\pm \pi^\mp \pi^+ \pi^-) = (7.03 \pm 2.10 \pm 0.70) \times 10^{-6}$. This measurement complements the previous BESIII measurement of $\psi(2S) \rightarrow$

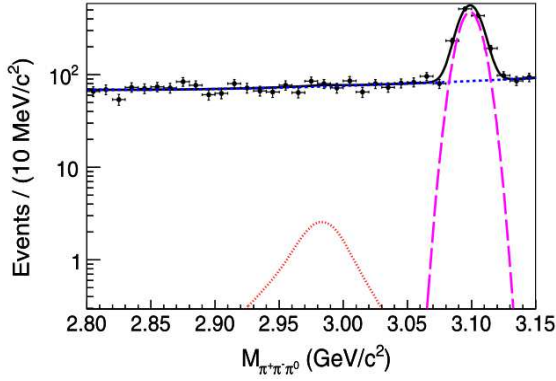


FIG. 9. Search for the isospin violation decay $\eta_c(1S) \rightarrow \pi^+\pi^-\pi^0$ via $\psi(2S) \rightarrow \gamma\eta_c(1S)$. The $\pi^+\pi^-\pi^0$ invariant mass distributions of the final candidate events in the $\eta_c(1S)$ mass region. The dots with error bars are data, the black solid line is the best fit, the red dashed line is $\eta_c(1S)$ signal, the long-dashed curve is the $J/\psi(1S)$ background, and the short-dashed curve is the main background [76].

$\gamma\eta_c(2S)$ with $\eta_c(2S) \rightarrow K_S^0 K^\pm \pi^\mp$ and $K^+ K^- \pi^0$ [86].

To compare with the BABAR results [7],

$$\frac{\mathcal{B}(\eta_c(2S) \rightarrow K^+ K^- \pi^+ \pi^- \pi^0)}{\mathcal{B}(\eta_c(2S) \rightarrow K_S^0 K^\pm \pi^\mp)} = 2.2 \pm 0.5 \pm 0.5, \quad (9)$$

we take the value of $(4.31 \pm 0.75) \times 10^{-6}$ as measured by BESIII for $\mathcal{B}(\psi(2S) \rightarrow \gamma\eta_c(2S)) \times \mathcal{B}(\eta_c(2S) \rightarrow K_S^0 K^\pm \pi^\mp)$ [86], and assuming that

$$\frac{\mathcal{B}(\eta_c(2S) \rightarrow K^+ K^- \pi^+ \pi^- \pi^0)}{\mathcal{B}(\eta_c(2S) \rightarrow K_S^0 K^\pm \pi^\mp \pi^+ \pi^-)} = 1.52, \quad (10)$$

where the value 1.52 is calculated in $\chi_{cJ}(1P)$ decays, which has the same isospin, we obtain

$$\begin{aligned} & \frac{\mathcal{B}(\eta_c(2S) \rightarrow K^+ K^- \pi^+ \pi^- \pi^0)}{\mathcal{B}(\eta_c(2S) \rightarrow K_S^0 K^\pm \pi^\mp)} \\ &= 1.52 \times \frac{\mathcal{B}(\eta_c(2S) \rightarrow K_S^0 K^\pm \pi^\mp \pi^+ \pi^-)}{\mathcal{B}(\eta_c(2S) \rightarrow K_S^0 K^\pm \pi^\mp)} \quad (11) \\ &= 2.48 \pm 0.56 \pm 0.33. \end{aligned}$$

These two results are consistent with each other after considering the statistical and systematic uncertainties.

With weighted least squares method [43], and combining statistical and systematic errors in quadrature, the averaged mass for $\eta_c(2S)$ at BESIII is calculated to be $(3641.45 \pm 2.53) \text{ MeV}/c^2$, and corresponding value of hyperfine splitting between 1S_0 and 3S_1 states is $\Delta M_{\text{hf}}(2S) = (44.69 \pm 2.53) \text{ MeV}/c^2$.

C. Search for $\eta_c(2S)$ in $\psi(2S) \rightarrow \gamma p\bar{p}$

In massless QCD models, the processes $\eta_c(1S)/\eta_c(2S)/\chi_{c0}(1P) \rightarrow p\bar{p}$ are forbidden by the helicity selection rule [89]. However, the experimental observations of the decay $\eta_c(1S)/\chi_{c0}(1P) \rightarrow p\bar{p}$ [3], indicate substantial contributions due to finite masses. These observations have stimulated many theoretical efforts [90–92]. In Ref. [93], it is pointed out that the BF of $\eta_c(2S) \rightarrow p\bar{p}$ with respect to that of $\eta_c(1P) \rightarrow p\bar{p}$ may serve as a criterion to validate the helicity conservation theorem, and an anomalous decay in $\eta_c(2S)$ might imply the existence of a glueball.

The decays $\eta_c(2S) \rightarrow p\bar{p}$ are searched for via $\psi(2S) \rightarrow \gamma p\bar{p}$, based on 448 million $\psi(2S)$ data sample. The invariant mass $p\bar{p}$ spectrum are shown in Fig. 10 (d). The fit yield 34 ± 17 for $\eta_c(2S) \rightarrow p\bar{p}$. The upper limits of the product BFs are determined to be $\mathcal{B}(\psi(2S) \rightarrow \gamma\eta_c(2S)) \times \mathcal{B}(\eta_c(2S) \rightarrow p\bar{p}) < 1.4 \times 10^{-6}$ at the 90% C.L. [94].

D. Search for $\eta_c(2S)$ decays into vector meson pairs

The decay modes $\eta_c(2S) \rightarrow VV$, are supposed to be highly suppressed by the helicity selection rule [95]. But in Ref. [96], a high production rate of $\eta_c(2S) \rightarrow VV$ is predicted, taking into consideration significant contributions from intermediate charmed meson loops, which provide a mechanism to evade helicity selection rule [62, 63]. The measurement of $\mathcal{B}(\eta_c(2S) \rightarrow VV)$ may help in understanding the role played by charmed meson loops in $\eta_c(1S) \rightarrow VV$.

The processes $\eta_c(2S) \rightarrow \rho^0 \rho^0, K^{*0} \bar{K}^{*0}$ and $\phi\phi$ are searched for using a sample of 1.06×10^8 $\psi(2S)$ events [97]. The final $\rho^0 \rho^0, K^{*0} \bar{K}^{*0}$ and $\phi\phi$ mass spectra and the fit results are shown in Fig. 11. No signal are observed in any of the three final states. The upper limits on the decay BFs are determined to be $\mathcal{B}(\eta_c(2S) \rightarrow \rho^0 \rho^0) < 3.1 \times 10^{-3}$, $\mathcal{B}(\eta_c(2S) \rightarrow K^{*0} \bar{K}^{*0}) < 5.4 \times 10^{-3}$, and $\mathcal{B}(\eta_c(2S) \rightarrow \phi\phi) < 2.0 \times 10^{-3}$ at 90% C.L.. The upper limits are lower than the existing theoretical predictions [96] where the predicted BFs are $\mathcal{B}(\eta_c(2S) \rightarrow \rho^0 \rho^0) = (6.4 \sim 28.9) \times 10^{-3}$, $\mathcal{B}(\eta_c(2S) \rightarrow K^{*0} \bar{K}^{*0}) = (7.9 \sim 35.8) \times 10^{-3}$ and $\mathcal{B}(\eta_c(2S) \rightarrow \phi\phi) = (2.1 \sim 9.8) \times 10^{-3}$, although the difference is very small for $\eta_c(2S) \rightarrow \phi\phi$.

V. $h_c(1P)$ PHYSICS

Since its discovery at CLEO experiment in 2005 [12, 13], few measurements of $h_c(1P)$ exclusive decay are available. Its dominate decay is the radiative transition $h_c(1P) \rightarrow \gamma\eta_c(1S)$ [98, 99], while the sum of the other known $h_c(1P)$ decay BFs is less than 3% [3].

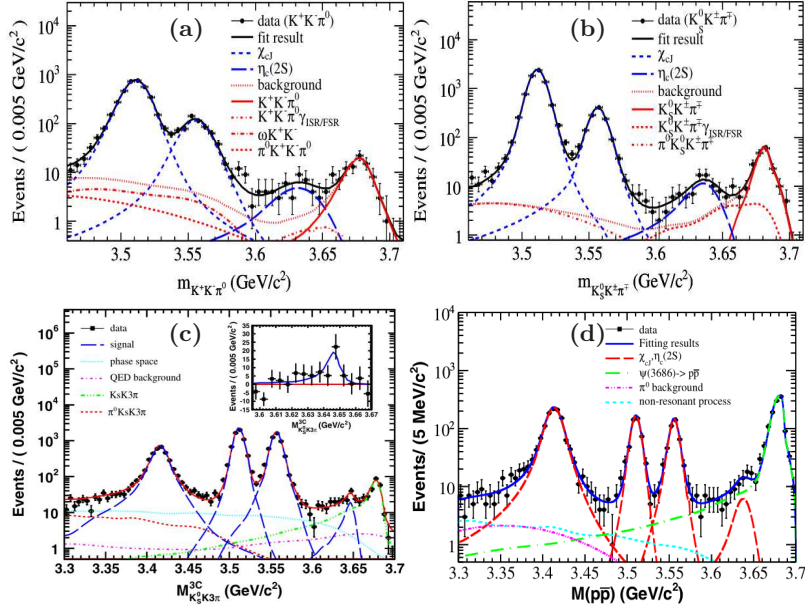


FIG. 10. First observation of the $M1$ transition $\psi(2S) \rightarrow \gamma\eta_c(2S)$ [86]: the invariant-mass spectra for $K_S^0 K^\pm \pi^\mp$ (a) and $K^+ K^- \pi^0$ (b), as well as the simultaneous fit; Evidence of $\eta_c(2S) \rightarrow K_S^0 K^\pm \pi^\mp \pi^+ \pi^-$ [88]: the invariant-mass spectra for $K_S^0 K^\pm \pi^\mp \pi^+ \pi^-$ (c); Search for $\eta_c(2S) \rightarrow p\bar{p}$ via $\psi(2S) \rightarrow \gamma p\bar{p}$ [94]: the invariant-mass spectra for $p\bar{p}$ (d), and the curves are total fit and each component.

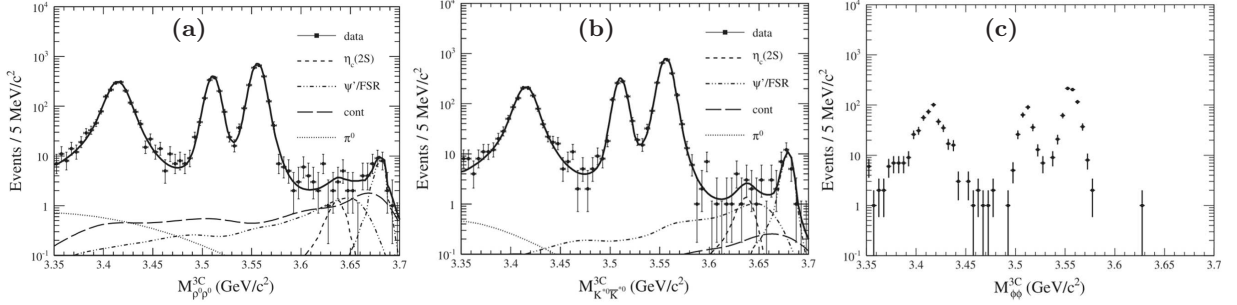


FIG. 11. Search for $\eta_c(2S)$ decays into vector meson pairs via $\psi(2S) \rightarrow \gamma\eta_c(2S)$ [97]. The fit to the invariant-mass spectra for $\rho^0 \rho^0$ (a), $K^{*0} \bar{K}^{*0}$ (b) and $\phi\phi$ (c). Dots with error bars are data, The curves in (a) and (b) are total fit and each component. No fit is performed for (c) due to low statistics.

A. $h_c(1P)$ resonance parameters

The properties of the $h_c(1P)$ are theoretically investigated in Refs. [100–103]. For example, Y. P. Kuang considered the effect of S - D mixing and predicted the $\mathcal{B}(\psi(2S) \rightarrow \pi^0 h_c(1P))$ to be $(0.4 - 1.3) \times 10^{-3}$, he also calculated the other BFs, e.g., $\mathcal{B}(h_c(1P) \rightarrow \gamma\eta_c(1S)) = 88\%$ and $\Gamma(h_c(1P)) = (0.51 \pm 0.01)$ MeV via PQCD and $\mathcal{B}(h_c(1P) \rightarrow \gamma\eta_c(1S)) = 41\%$ and $\Gamma(h_c(1P)) = (1.1 \pm 0.09)$ MeV via nonrelativistic QCD (NRQCD). Godfrey and Rosner gave a different theoretical prediction, $\mathcal{B}(h_c(1P) \rightarrow \gamma\eta_c(1S)) = 38\%$ [104]. A recent unquenched LQCD analysis predicted the width $\Gamma(h_c(1P)) = (0.601 \pm 0.055)$ MeV [105].

The precise measurement to $h_c(1P)$ resonant parameters is important because the comparison of its mass with

the 3P states ($\chi_{cJ}(1P)$) provides an essential information about the spin dependence of the $c\bar{c}$ interaction, which can be obtained by precisely measuring the 1P hyperfine mass splitting $\Delta M_{\text{hf}}(1P) \equiv \langle M(1^3P) \rangle - M(1^1P_1)$, where $\langle M(1^3P_J) \rangle = [M(\chi_{c0}) + 3M(\chi_{c1}) + 5M(\chi_{c2})]/9 = 3525.30 \pm 0.04$ MeV/ c^2 [106] is the spin-weighted centroid of the 3P_J mass and $M(1^1P_1)$ is the mass of the singlet state $h_c(1P)$. A non-zero hyperfine splitting may give indication of non-vanishing spin-spin interactions in charmonium potential models [107].

According to QCD potential models, the $c\bar{c}$ interaction in a charmonium meson can be described with a potential that includes a Lorentz scalar confinement term and a vector Coulombic term arising from one-gluon exchange between the quark and the antiquark. The scalar confining potential makes no contribution to the hyperfine

interaction and the Coulombic vector potential produces hyperfine splitting only for S states. This leads to the prediction of the hyperfine or triplet-singlet splitting in the P states of $\Delta M_{\text{hf}}(1P) \equiv \langle M(1^3P) \rangle - M(1^1P_1) \simeq 0$ [107].

The decay mode of $\psi(2S) \rightarrow \pi^0 h_c(1P)$ is studied using three methods at BESIII: (1) just tagging the π^0 , called inclusive method [108]; (2) tagging the π^0 and $E1$ gamma in the $E1$ transition decay $h_c(1P) \rightarrow \gamma \eta_c(1S)$, called $E1$ tagging method [108]; (3) reconstruct $\eta_c(1S)$ with 16 exclusive hadronic decays, called exclusive method [36].

The π^0 recoil-mass spectrum obtained with inclusive method and $E1$ tagging method, as well as the fitting status, are shown in Fig. 12. The corresponding event numbers of $\eta_c(1S)$ signal observed are 10353 ± 1097 and 3679 ± 319 , respectively.

The absolute BFs $\mathcal{B}(\psi(2S) \rightarrow \pi^0 h_c(1P)) = (8.4 \pm 1.3 \pm 1.0) \times 10^{-4}$ and $\mathcal{B}(h_c(1P) \rightarrow \gamma \eta_c(1S)) = (54.3 \pm 6.7 \pm 5.2)\%$ are measured for the first time. A statistics-limited determination of the previously unmeasured $h_c(1P)$ width leads to an upper limit $\Gamma(h_c(1P)) < 1.44$ MeV (90% C.L.). The measured $M(h_c(1P)) = 3525.40 \pm 0.13 \pm 0.18$ MeV/ c^2 and $\mathcal{B}(\psi(2S) \rightarrow \pi^0 h_c(1P)) \times \mathcal{B}(h_c(1P) \rightarrow \gamma \eta_c(1S)) = (4.58 \pm 0.40 \pm 0.50) \times 10^{-4}$ are consistent with previous results [99]. The measured $\mathcal{B}(h_c(1P) \rightarrow \gamma \eta_c(1S))$ is close to the prediction in Ref. [104] (38%) and the NRQCD prediction of Ref. [103]. The measured $\mathcal{B}(\psi(2S) \rightarrow \pi^0 h_c(1P))$ is consistent with the prediction of Ref. [103], and the total width $\Gamma(h_c)$ is consistent with the predictions of Ref. [103, 105]. The $1P$ hyperfine mass splitting to be $\Delta M_{\text{hf}} \equiv \langle M(1^3P) \rangle - M(1^1P_1) = -0.10 \pm 0.13 \pm 0.18$ MeV/ c^2 , consistent with no strong spin-spin interaction.

The π^0 recoil-mass spectrum summed over the 16 final states, as well as the fitting status, obtained with exclusive method are shown in Fig. 13.

The measured mass and width, $M(h_c(1P)) = (3525.31 \pm 0.11 \pm 0.14)$ MeV/ c^2 and $\Gamma(h_c(1P)) = (0.70 \pm 0.28 \pm 0.22)$ MeV, are consistent with previous measurements by $\eta_c(1S)$ inclusive decay.

With weighted least squares method [43], and combining statistical and systematic errors in quadrature, the averaged mass for $h_c(1P)$ at BESIII is (3525.35 ± 0.14) MeV/ c^2 , and the mass splitting with P wave iso-spin triplet is $\Delta M_{\text{hf}}(1P) = (-0.05 \pm 0.15)$ MeV/ c^2 which is consistent with zero with one standard deviation and not violates the assumption that there is only short-distance contribution in potential model [107].

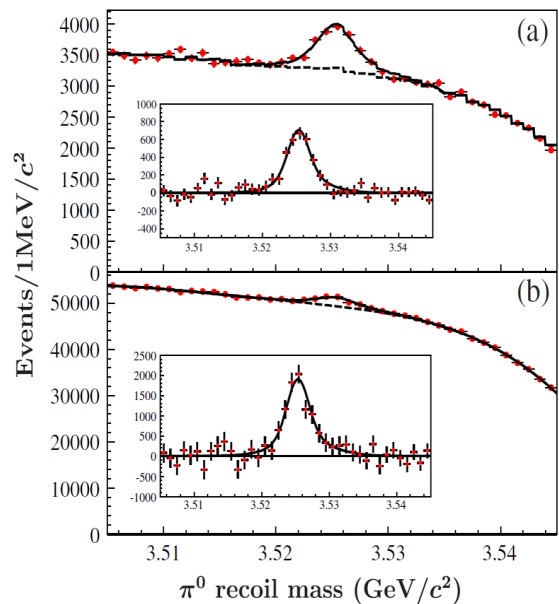


FIG. 12. Measurements of $h_c(1P)$ in $\psi(2S)$ decays. (a) The π^0 recoil-mass spectrum and fit for the $E1$ -tagged analysis of $\psi(2S) \rightarrow \pi^0 h_c(1P)$, $h_c(1P) \rightarrow \gamma \eta_c(1S)$. (b) The π^0 recoil-mass spectrum and fit for the inclusive analysis of $\psi(2S) \rightarrow \pi^0 h_c(1P)$. Fits are shown as solid lines, background as dashed lines. The insets show the background-subtracted spectra [108].

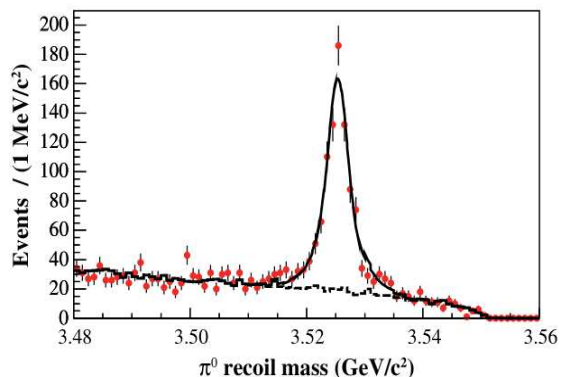


FIG. 13. Study of $\psi(2S) \rightarrow \pi^0 h_c(1P)$, $h_c(1P) \rightarrow \gamma \eta_c(1S)$ via $\eta_c(1S)$ exclusive decays. The π^0 recoil mass spectrum in $\psi(2S) \rightarrow \pi^0 h_c(1P)$, $h_c(1P) \rightarrow \gamma \eta_c(1S)$, $\eta_c(1S) \rightarrow X_i$ summed over the 16 final states X_i . The dots with error bars represent the π^0 recoil mass spectrum in data. The solid line shows the total fit function and the dashed line is the background component of the fit [36].

B. $h_c(1P)$ decays

1. Observation of $h_c(1P) \rightarrow \gamma \eta'$ and evidence for $h_c(1P) \rightarrow \gamma \eta$

Since the $h_c(1P)$ has negative C parity, it very likely decays into a photon plus a pseudoscalar meson, such

as η and η' . The η and η' mesons are commonly understood as mixtures of the pure SU(3) flavor octet $[(u\bar{u} + d\bar{d} - 2s\bar{s})/\sqrt{6}]$ and singlet $[(u\bar{u} + d\bar{d} + s\bar{s})/\sqrt{3}]$ states and a small gluonium component [109] [110]. The flavor content of each $\eta^{(\prime)}$ mass eigenstate can be quantified with a mixing angle, the value of which becomes manifest in ratios of branching fractions for various radiative decays involving a η or η' [111] [112] [113]. The ratio of the BF $\mathcal{B}(h_c(1P) \rightarrow \gamma\eta)$ over $\mathcal{B}(h_c(1P) \rightarrow \gamma\eta')$ can be used to study the $\eta - \eta'$ mixing angle, and is also important to test SU(3)-flavor symmetries in QCD [114]. As in the case of ψ (including J/ψ and $\psi(2S)$) decays, the process $\psi \rightarrow \gamma\eta$ and $\psi \rightarrow \gamma\eta'$ occur primarily through radiative of the photon from the c quark or \bar{c} quark in the initial state. Assuming such a mechanism and the applicability of SU(3) symmetry for the decay amplitudes, the decay proceeds through the SU(3)-singlet part of the pseudoscalar. One finds [115]

$$\frac{\Gamma(\psi \rightarrow \gamma\eta')}{\Gamma(\psi \rightarrow \gamma\eta)} = \left(\frac{k_{\eta'}}{k_{\eta}}\right)^3 \frac{1}{\tan^2\theta}, \quad (12)$$

The radiative decay process $h_c(1P) \rightarrow \gamma\eta'$ is observed with a statistical significance of 8.4σ for the first time, and the evidence for the process $h_c(1P) \rightarrow \gamma\eta$ with a significance of 4.0σ [116] at BESIII. Here, η' is reconstructed with $\eta\pi^+\pi^-$ and $\gamma\pi^+\pi^-$ modes, while η is reconstructed with $\gamma\gamma$ and $\pi^+\pi^-\pi^0$ modes. Figure 14 shows the distributions of $M(\gamma\eta')$ and $M(\gamma\eta)$ for the selected events. The corresponding BFs of $h_c(1P) \rightarrow \gamma\eta'$ and $h_c(1P) \rightarrow \gamma\eta$ are measured to be $(1.52 \pm 0.27 \pm 0.29) \times 10^{-3}$ and $(4.7 \pm 1.5 \pm 1.4) \times 10^{-4}$, respectively, where the first errors are statistical and the second are systematic. The ratio of $\mathcal{B}(h_c(1P) \rightarrow \gamma\eta)$ over $\mathcal{B}(h_c(1P) \rightarrow \gamma\eta')$ is $R_{h_c(1P)} = \mathcal{B}(h_c(1P) \rightarrow \gamma\eta)/\mathcal{B}(h_c(1P) \rightarrow \gamma\eta') = (30.7 \pm 11.3 \pm 8.7)\%$, where the common systematic errors between $\mathcal{B}(h_c(1P) \rightarrow \gamma\eta)$ and $\mathcal{B}(h_c(1P) \rightarrow \gamma\eta')$ cancel. The $\eta - \eta'$ mixing angle can be extracted from $R_{h_c(1P)}$ to test SU(3)-flavor symmetries in QCD [114], following the methods used for equivalent decays of the ψ mesons [117–119].

2. Measurement of $h_c(1P) \rightarrow$ light hadrons

For the $h_c(1P)$ hadronic decays, the predictions on the ratios of hadronic with of the $h_c(1P)$ to that of $\eta_c(1S)$, based on the PQCD and NRQCD are very different [101]. Assuming that

$$\frac{\Gamma(h_c(1P) \rightarrow h)}{\Gamma(\eta_c(1S) \rightarrow h)} \approx \frac{\Gamma(h_c(1P) \rightarrow 3g)}{\Gamma(\eta_c(1S) \rightarrow 2g)}, \quad (13)$$

and taking into account of

$$\frac{\Gamma(\eta_c(1S) \rightarrow 2g)}{\Gamma(J/\psi(1S) \rightarrow 3g)} = \frac{27}{5(\pi^2 - 9)\alpha_s} \left(\frac{M_{J/\psi(1S)}^2}{M_{\eta_c(1S)}^2}\right), \quad (14)$$

$\Gamma(h_c(1P) \rightarrow h)/\Gamma(\eta_c(1S) \rightarrow h)$ is calculated to be 0.010 ± 0.001 in PQCD, while 0.083 ± 0.018 in NRQCD, as is the corresponding ratio involving decays of $J/\psi(1S)$ mesons ($\Gamma_{h_c(1P)}^{\text{had.}}/\Gamma_{J/\psi(1S)}^{\text{had.}}$). New studies of $h_c(1P)$ hadronic decays will enable these ratios to be measured, and comparisons to be made with the theoretical predictions. Fifteen $h_c(1P)$ exclusive hadronic decays as listed in Table. V, are searched for via the process $\psi(2S) \rightarrow \pi^0 h_c(1P)$ [120, 121] at BESIII. Four of them, $h_c(1P) \rightarrow p\bar{p}\pi^+\pi^-$, $h_c(1P) \rightarrow \pi^+\pi^-\pi^0$, $2(\pi^+\pi^-\pi^0)$ and $K^+K^-\pi^+\pi^-\pi^0$ are observed for the first time with significance of 7.4σ , 4.6σ , 9.1σ and 6.0σ . Evidences for the decays $h_c(1P) \rightarrow \pi^+\pi^-\pi^0\eta$ and $h_c(1P) \rightarrow K_S^0 K^\pm \pi^\mp \pi^+\pi^-$ is found with a significance of 3.6σ and 3.8σ , respectively. The invariant mass for these final states and the fit status are shown in Fig. 15, 16. The corresponding BRs (and upper limits) are summarized in Table. V.

Table VI shows the comparisons of the measured ratios of the hadronic decay widths $\Gamma_{h_c(1P)}^{\text{had.}}/\Gamma_{\eta_c(1S)}^{\text{had.}}$ and $\Gamma_{h_c(1P)}^{\text{had.}}/\Gamma_{J/\psi(1S)}^{\text{had.}}$ and the theoretical predictions. The experimental results tend to favor the lower predictions, which come from pQCD. However, in Ref. [103], the theoretical prediction of $\mathcal{B}(h_c(1P) \rightarrow \gamma\eta_c(1S)) = (41 \pm 3)\%$ based on NRQCD is favored by the experimental measurement $(51 \pm 6)\%$ [3], compared with the prediction of $(88 \pm 2)\%$ from pQCD. We note that the experimental measurements are still limited by low statistics and the predictions of the theoretical models can be modified through considerations such as normalization scale or relativistic corrections [122] [123]. Future experimental measurements of higher precision, and improved theoretical calculations will help to resolve this inconsistency.

3. Search for $h_c(1P) \rightarrow \pi^+\pi^- J/\psi$

Hadronic transitions between the heavy quarkonium ($Q\bar{Q}$) states are particularly interesting for testing the interplay between PQCD and NPQCD [124]. A common approach for calculating these transitions is the QCD multipole expansion [125] for gluon emission. The calculation depends on experimental inputs and works well for transitions of heavy $Q\bar{Q}$ states below open flavor threshold [126]. However to date, the only well-measured hadronic transitions in the charmonium sector are those for the $\psi(2S)$.

For charmonium states below the $D\bar{D}$ threshold, the hadronic transitions of the spin-singlet P-wave state $h_c(1P)$ are one of the best places to test the spin-spin interaction between heavy quarks [127], but they remain the least accessible experimentally because the h_c cannot be produced resonantly in e^+e^- annihilation or from electric-dipole radiative transitions of the $\psi(2S)$.

The $h_c(1P)$ is expected to decay to lower-mass charmonium state through hadronic transitions, but this has not been observed yet. In the framework of QCDME,

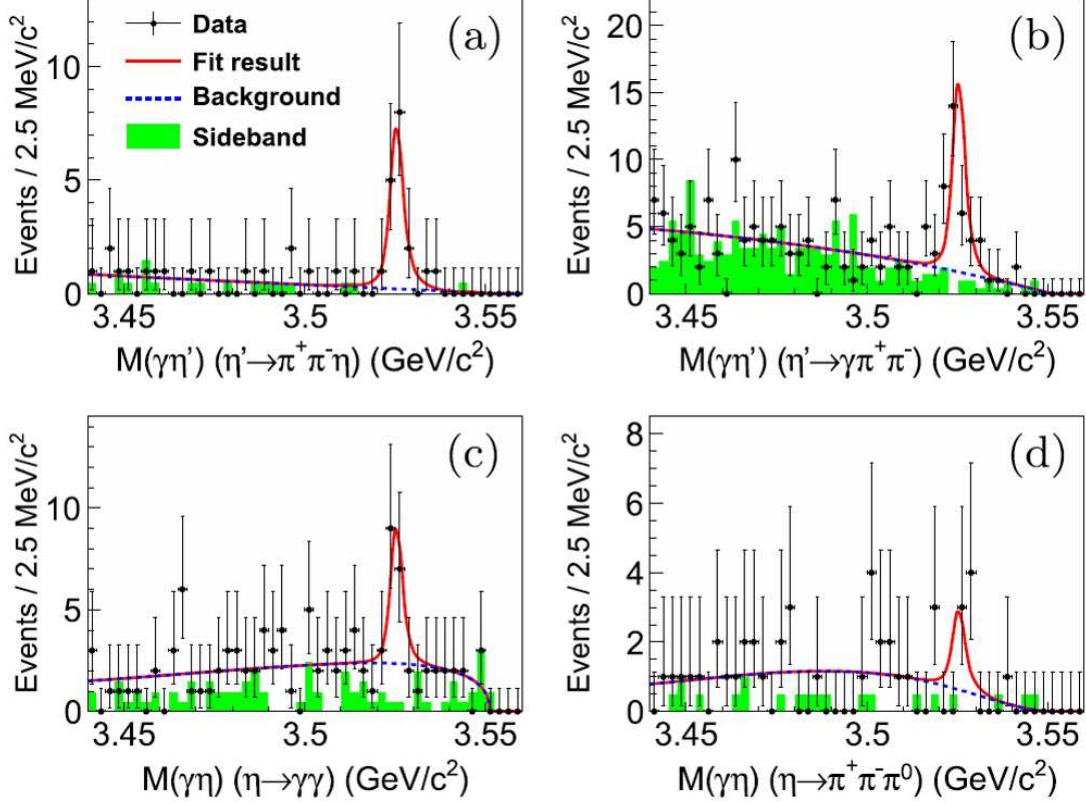


FIG. 14. Observation of $h_c(1P) \rightarrow \gamma \eta'$ and evidence for $h_c(1P) \rightarrow \gamma \eta$ [116]. Results of the simultaneous fits to the two invariant mass distributions of (top) $M(\gamma \eta')$ and (below) $M(\gamma \eta)$ for data. (a) $M(\gamma \eta')$ distribution for $h_c(1P) \rightarrow \gamma \eta'$ ($\eta' \rightarrow \pi^+ \pi^- \eta$). (b) $M(\gamma \eta')$ distribution for $h_c(1P) \rightarrow \gamma \eta'$ ($\eta' \rightarrow \gamma \pi^+ \pi^-$). (c) $M(\gamma \eta)$ distribution for $h_c(1P) \rightarrow \gamma \eta$ ($\eta \rightarrow \gamma \gamma$). (d) $M(\gamma \eta)$ distribution for $h_c(1P) \rightarrow \gamma \eta$ ($\eta \rightarrow \pi^+ \pi^- \pi^0$). The red solid curves are the fit results, the blue dashed curves are the background distributions, and the green hatched histograms are events from the $\eta(\eta')$ sidebands.

TABLE V. Review of the measured BF of $h_c(1P) \rightarrow X$ at BESIII. Here, X denotes hadronic final states, ϵ denotes the selection efficiency, $N_{h_c(1P)}$ denotes the $h_c(1P)$ signal yield. \mathcal{B} denote the BF $\mathcal{B}(h_c(1P) \rightarrow \text{hadrons})$. S.S. is the significance of the signal peak, including systematic uncertainties. The last column gives the status before the BESIII experiment.

| Decay mode | X | Yield | $\epsilon(\%)$ | $\mathcal{B}(10^{-3})$ | S.S. | Ref. | Comment |
|------------|---|--------------|----------------|--------------------------|-------------|-------|-------------------|
| (I) | $h_c(1P) \rightarrow p\bar{p}\pi^+\pi^-$ | 230 ± 25 | 20.9 | $2.89 \pm 0.32 \pm 0.55$ | 7.4σ | [120] | first measurement |
| (II) | $h_c(1P) \rightarrow \pi^+\pi^-\pi^0$ | 101 ± 25 | 16.8 | $1.60 \pm 0.40 \pm 0.32$ | 4.6σ | [120] | < 2.2 |
| (III) | $h_c(1P) \rightarrow 2(\pi^+\pi^-)\pi^0$ | 254 ± 32 | 9.1 | $7.44 \pm 0.94 \pm 1.52$ | 9.1σ | [120] | 22^{+8}_{-7} |
| (IV) | $h_c(1P) \rightarrow 3(\pi^+\pi^-)\pi^0$ | 73 ± 34 | 4.2 | $4.65 \pm 2.17 \pm 1.08$ | 2.1σ | [120] | < 29 |
| | | < 136 | | < 8.7 | | | |
| (V) | $h_c(1P) \rightarrow K^+K^-\pi^+\pi^-$ | < 40 | 18.1 | < 0.6 | ... | [120] | first measurement |
| (i) | $h_c(1P) \rightarrow K^+K^-\pi^+\pi^-\pi^0$ | 80 ± 15 | 6.5 | $3.3 \pm 0.6 \pm 0.6$ | 6.0σ | [121] | first measurement |
| (ii) | $h_c(1P) \rightarrow \pi^+\pi^-\pi^0\eta$ | 35 ± 9 | 3.3 | $7.2 \pm 1.8 \pm 1.3$ | 3.6σ | [121] | first measurement |
| | | < 50.0 | | < 18 | | | |
| (iii) | $h_c(1P) \rightarrow K_S^0 K^\pm \pi^\mp \pi^+ \pi^-$ | 41 ± 13 | 5.5 | $2.8 \pm 0.9 \pm 0.5$ | 3.8σ | [121] | first measurement |
| | | < 65.3 | | < 4.7 | | | |
| (iv) | $h_c(1P) \rightarrow K^+K^-\pi^0$ | < 20.1 | 9.8 | < 0.6 | ... | [121] | first measurement |
| (v) | $h_c(1P) \rightarrow K^+K^-\eta$ | < 18.5 | 14.3 | < 0.9 | ... | [121] | first measurement |
| (vi) | $h_c(1P) \rightarrow K^+K^-\pi^+\pi^-\eta$ | < 24.1 | 6.9 | < 2.5 | ... | [121] | first measurement |
| (vii) | $h_c(1P) \rightarrow 2(K^+K^-\pi^0)$ | < 11.7 | 6.7 | < 0.3 | ... | [121] | first measurement |
| (viii) | $h_c(1P) \rightarrow K^+K^-\pi^0\eta$ | < 20.2 | 6.3 | < 2.2 | ... | [121] | first measurement |
| (ix) | $h_c(1P) \rightarrow K_S^0 K^\pm \pi^\mp$ | < 17.4 | 14.4 | < 0.6 | ... | [121] | first measurement |
| (x) | $h_c(1P) \rightarrow p\bar{p}\pi^0\pi^0$ | < 11.8 | 8.7 | < 0.5 | ... | [121] | first measurement |

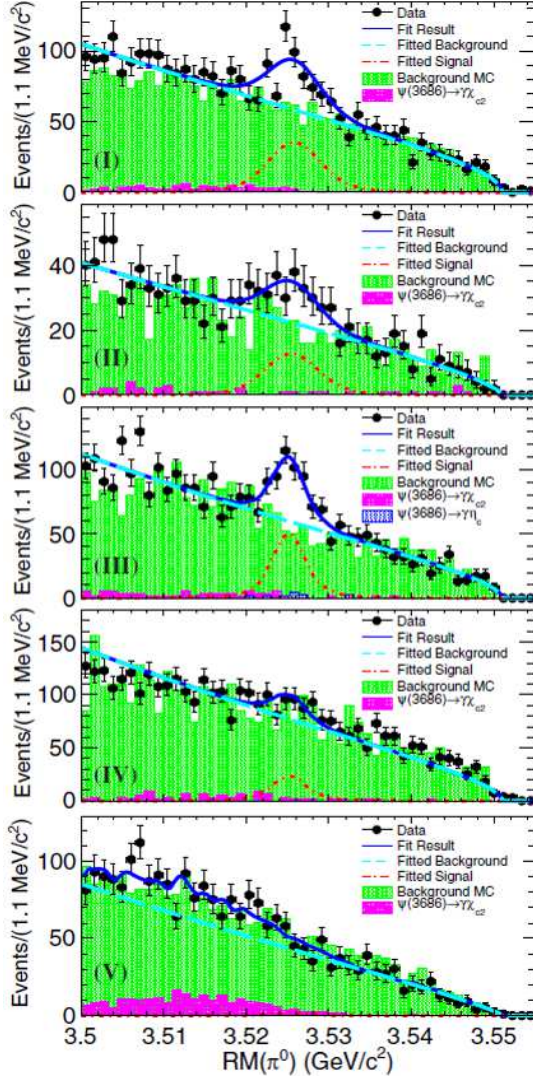


FIG. 15. Observation of $h_c(1P) \rightarrow$ hadrons. Recoiling mass spectra of the lowest energy π^0 , in the decay chains $\psi(2S) \rightarrow \pi^0 h_c(1P)$ with $h_c(1P) \rightarrow p\bar{p}\pi^+\pi^-$ (I), $\pi^+\pi^-\pi^0$ (II), $2(\pi^+\pi^-)\pi^0$ (III), $3(\pi^+\pi^-)\pi^0$ (IV), and $K^+K^-\pi^+\pi^-$ (V). In each spectrum, the dots with error bars represent data, the pink shaded histogram is the background process $\psi(2S) \rightarrow \gamma\chi_{c2}(1P)$, the blue filled histogram is the background process $\psi(2S) \rightarrow \pi^0 h_c(1P)$, $h_c(1P) \rightarrow \gamma\eta_c(1S)$, the green filled histogram is the background from inclusive MC, the cyan dashed curve is the fitted background, the red dash-dotted curve is the fitted signal, and the blue curve is the fitted result [120].

the BF of $h_c(1P) \rightarrow \pi\pi J/\psi(1S)$ (including charged and neutral modes) is predicted to be 2% [128], while it is predicted to be 0.05% when neglecting the nonlocality in time [129]. An experimental measurement is desirable to distinguish between these calculations.

A search for the hadronic transition $h_c(1P) \rightarrow \pi^+\pi^- J/\psi(1S)$ is carried out via $\psi(2S) \rightarrow \pi^0 h_c(1P)$, $h_c(1P) \rightarrow \pi^+\pi^- J/\psi(1S)$ at BESIII [130]. No signal

TABLE VI. The ratios of hadronic decay width of $h_c(1P)$ to $\eta_c(1S)$ ($\Gamma_{h_c(1P)}^{\text{had.}}/\Gamma_{\eta_c(1S)}^{\text{had.}}$) and $h_c(1P)$ to $J/\psi(1S)$ ($\Gamma_{h_c(1P)}^{\text{had.}}/\Gamma_{J/\psi(1S)}^{\text{had.}}$). The theoretical predictions of the total hadronic decay ratios are based on pQCD and NRQCD [103], which are expected to be correct also for exclusive decay modes. The experimental measurements of the ratios of the partial decay widths for $p\bar{p}\pi^+\pi^-$, $K^+K^-\pi^+\pi^-$, and $n(\pi^+\pi^-)\pi^0$ ($n = 0, 1, 2$) modes are calculated based on the measured branching fractions in Ref. [120] [121] and the PDG [3].

| | Model/mode | Ratio |
|--|--|-------------------|
| $\Gamma_{h_c(1P)}^{\text{had.}}/\Gamma_{\eta_c(1S)}^{\text{had.}}$ | PQCD | 0.010 ± 0.001 |
| | NRQCD | 0.083 ± 0.018 |
| | $p\bar{p}\pi^+\pi^-$ | 0.012 ± 0.008 |
| | $K^+K^-\pi^+\pi^-$ | < 0.002 |
| | $K^+K^-\pi^+\pi^-\pi^0$ | 0.002 ± 0.001 |
| | $K_S^0 K^\pm \pi^\mp$ | < 0.001 |
| | $K_S^0 K^\pm \pi^\mp \pi^\pm \pi^\mp$ | < 0.002 |
| | $K^+K^-\pi^0$ | < 0.001 |
| | $K^+K^-\eta$ | < 0.001 |
| | $\Gamma_{h_c(1P)}^{\text{had.}}/\Gamma_{J/\psi(1S)}^{\text{had.}}$ | PQCD |
| NRQCD | | 8.03 ± 1.31 |
| $p\bar{p}\pi^+\pi^-$ | | 3.63 ± 2.25 |
| $\pi^+\pi^-\pi^0$ | | 0.57 ± 0.38 |
| $2(\pi^+\pi^-)\pi^0$ | | 1.43 ± 0.90 |
| $3(\pi^+\pi^-)\pi^0$ | | < 2.26 |
| $K^+K^-\pi^+\pi^-$ | | < 0.66 |
| $K^+K^-\pi^0$ | | < 2.35 |
| $K_S^0 K^\pm \pi^\mp$ | | < 0.81 |
| $K^+K^-\pi^+\pi^-\pi^0$ | | 2.07 ± 1.40 |
| $K^+K^-\pi^+\pi^-\eta$ | < 4.0 | |

is observed. The upper limit of the product of BFs $\mathcal{B}(\psi(2S) \rightarrow \pi^0 h_c(1P)) \mathcal{B}(h_c(1P) \rightarrow \pi^+\pi^- J/\psi(1S))$ at the 90% C.L. is determined to be 2.0×10^{-6} . Using the PDG value for the BF of $\psi(2S) \rightarrow \pi^0 h_c(1P)$ of $(8.6 \pm 1.3) \times 10^{-4}$ [3], the upper limit on $\mathcal{B}(h_c(1P) \rightarrow \pi^+\pi^- J/\psi(1S))$ is determined to be 2.4×10^{-3} , which is the most stringent upper limit to date. Neglecting the small phase space difference between the charged and neutral $\pi\pi$ modes and assuming isospin symmetry, upper limit for $\mathcal{B}(h_c(1P) \rightarrow \pi\pi J/\psi(1S))$ at 90% C.L. is determined to be 3.6×10^{-3} (including charged and neutral modes). It is noted that the measured BF is smaller than the prediction in Ref. [128] by one order in magnitude, but does not contradict that in Ref. [129].

VI. SUMMARY AND PROSPECTIVES

With the capability of adjusting the e^+e^- c.m. energy to the peaks of resonances, combined with the clean experimental environments due to near-threshold operation, BESIII is uniquely able to perform a broad range of critical measurements of charmonium physics, as discussed above in the context of the studies of $\eta_c(1S)$,

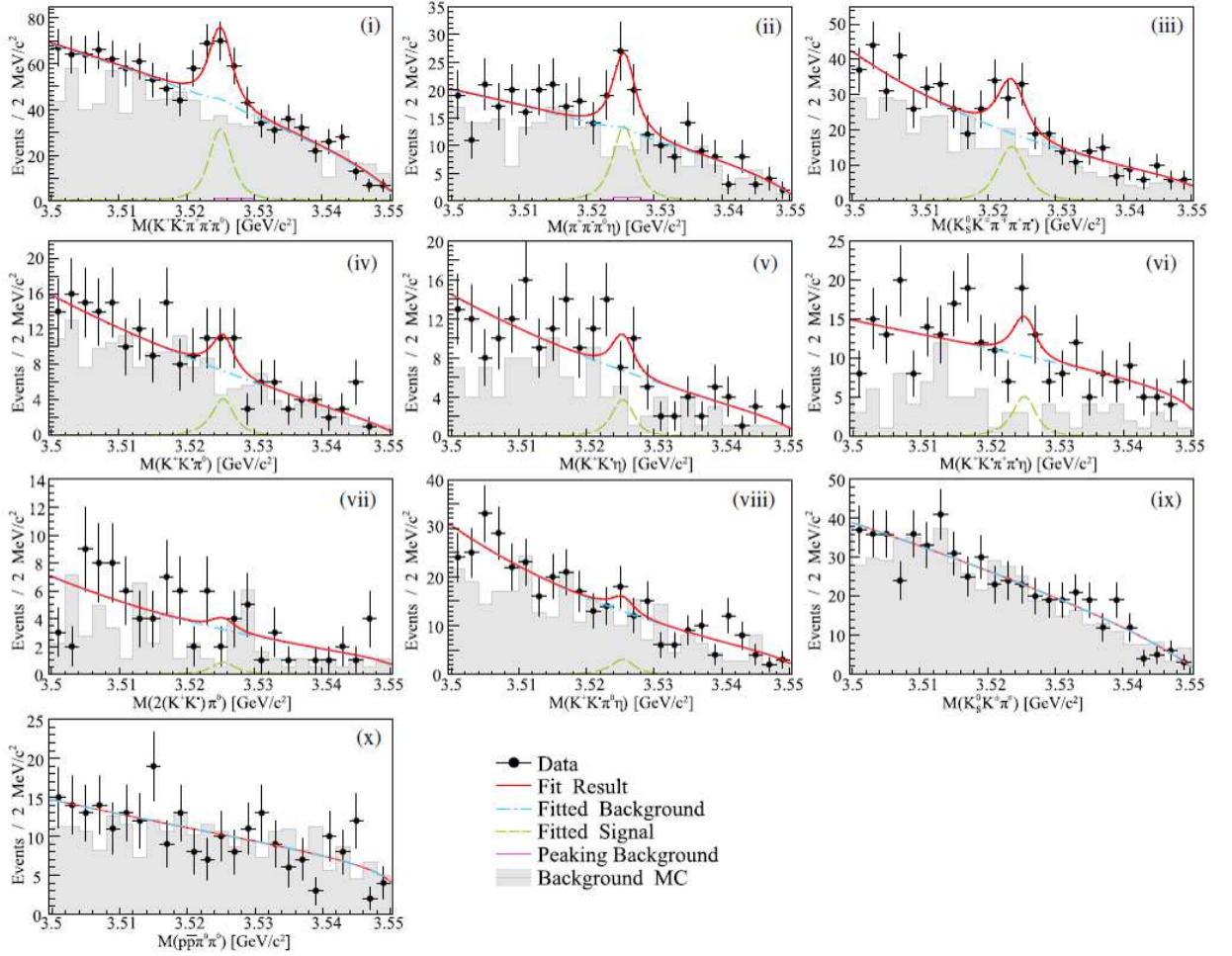


FIG. 16. Observation of $h_c(1P) \rightarrow K^+K^-\pi^+\pi^-\pi^0$. Fits to the invariant mass distributions for the h_c decay modes (i)-(x). Data are shown as black points, the total fit result is shown in red, the background contribution is denoted by the blue dashed-dotted line (including peaking background contributions for channel (i) and (ii) as shown in magenta), the signal contribution is illustrated by the green dashed line. The background level obtained from inclusive MC is shown by the gray shaded histogram [121].

$\eta_c(2S)$ and $h_c(1P)$ states.

Despite the impressive progress, many $\eta_c(1S)$, $\eta_c(2S)$ and $h_c(1P)$ decays are still to be observed and explored.

At present, the BESIII detector has collected the world's largest $J/\psi(1S)$ data sample of $N_{J/\psi(1S)} = (10087 \pm 44) \times 10^6$ [131]. In addition, BESIII has collected a sample of 2.55×10^9 $\psi(2S)$ data sample in this year. Thus, there will be about 3.0×10^9 $\psi(2S)$ data sample in total. BESIII also has a great plan for collecting the XYZ data sample [1].

With these unique advantage of an unprecedented high-statistics data samples, the BESIII experiment could further study the $\eta_c(1S)$, $\eta_c(2S)$ and $h_c(1P)$ state in the following aspects.

1. Give more precise measurements of the masses and widths of the $\eta_c(1S)$ and $h_c(1P)$ via $E1$ transition $h_c(1P) \rightarrow \gamma\eta_c(1S)$ because of the negligible interference

and $\eta_c(2S)$ via the $M1$ transition $\psi(2S) \rightarrow \gamma\eta_c(2S)$ with statistical uncertainty reduced significantly, and better understand the line shapes associated with their production, to precisely test the predicted hyperfine mass splitting based on the potential models [107], and recent lattice computations [37–39], as well as quark-model predictions [40].

2. Give more precise measurement for their known hadronic decay modes, and investigate more decay modes of the $\eta_c(1S)$, $\eta_c(2S)$ and $h_c(1P)$ states to test the predictions on the ratios of hadronic width of the $h_c(1P)$ to that of $\eta_c(1S)$, and the ratios of hadronic decay width of $h_c(1P)$ to that of $J/\psi(1S)$, based on pQCD and NRQCD [103]. For instance, $h_c(1P) \rightarrow p\bar{p}\pi^+\pi^-\pi^0$, $p\bar{p}\eta$ and $p\bar{p}\pi^0$, $\eta_c(2S) \rightarrow \pi^+\pi^-\eta$, and so on.

3. Search for the Di-pion transition decays $\eta_c(2S) \rightarrow \eta_c(1S)\pi^+\pi^-$ and $h_c(1P) \rightarrow \pi^+\pi^-J/\psi(1S)$. In particular, the Di-pion transition amplitude for $\eta_c(2S) \rightarrow$

$\eta_c(1S)\pi^+\pi^-$ is expected [132] to have the same approximately linear dependence on the squared invariant mass of the di-pion system as the $\psi(2S) \rightarrow J/\psi(1S)\pi^+\pi^-$ [133]. PHSP integration of the squared amplitude, evaluated for the peak masses $M_{\eta_c(1S)}$ and $M_{\eta_c(2S)}$ of the $\eta_c(1S)$ and $\eta_c(2S)$, respectively, yields $\Gamma(\eta_c(2S) \rightarrow \eta_c(1S)\pi^+\pi^-)/\Gamma(\psi(2S) \rightarrow J/\psi(1S)\pi^+\pi^-) \approx 2.9$. This will lead to the BF prediction $\mathcal{B}(\eta_c(2S) \rightarrow \eta_c(1S)\pi^+\pi^-) = (2.2_{-0.6}^{+1.6})\%$. This decay may be further suppressed due to the contribution of the chromomagnetic interaction to the decay amplitude [134]. However, it is not observed yet in experiment yet [135] [136], and only the upper limit of its branching fraction is determined and to be $\mathcal{B}(\eta_c(2S) \rightarrow \eta_c(1S)\pi^+\pi^-) < 25\%$ [3].

4. Study the electromagnetic (EM) Dalitz decay $h_c(1P) \rightarrow e^+e^-\eta_c(1S)$ and $J/\psi(1S)/\psi(2S) \rightarrow e^+e^-\eta_c(1S)$, which have access to the EM transition form factors (TFFs) of these charmonium states. The q^2 dependence of charmonium TFFs can provide additional information of the interactions between the charmonium states and the electromagnetic field, where q^2 is the square of the invariant mass of the e^+e^- pair, and serve as a sensitive probe to their internal structures. Furthermore, the q^2 -dependent TFF can possibly distinguish the transition mechanisms based on the $c\bar{c}$ scenario and other solutions which alter the simple quark model picture.

5. Study the $\eta_c(1S)$ state via the M1 transition to improve the precision of $\mathcal{B}(\psi(2S) \rightarrow \gamma\eta_c(1S))$, and the $\eta_c(2S)$ state with $\mathcal{B}(\psi(2S) \rightarrow \gamma\eta_c(2S))$ which could be used to extract the absolute BFs for some specific $\eta_c(2S)$ decays. There are other radiative transitions such as $\eta_c(2S) \rightarrow \gamma J/\psi(1S)$, $\eta_c(2S) \rightarrow \gamma h_c(1P)$, $\chi_{c2}(1P) \rightarrow \gamma h_c(1P)$, and $h_c(1P) \rightarrow \gamma\chi_{c0,1}(1P)$ that are challenges for BESIII even with 10^9 $\psi(2S)$ data sample because of low decay rates or difficulty in detecting the soft photon, but these rates can be calculated in the potential model [137] and experimental searches are therefore important.

6. Study the radiative decays of the charmonium states for a better understanding of charmonium decay dynamics, such as $\eta_c(1S) \rightarrow \gamma V$ with the predicted BR in the level of $10^{-6} \sim 10^{-7}$ in the framework of NRQCD [138]. And the improved measurement of $\eta_c(1S) \rightarrow \gamma\gamma$ will shed

light on the effects of higher order QCD corrections as well as provide validation of the decoupling of the hard and soft contributions in the NRQCD framework due to its simplicity [139]. With the larger data samples, all of these measurements will be improved.

7. Study the two-body baryonic decays of the $\eta_c(1S)$, $\eta_c(2S)$ and $h_c(1P)$, which can provide information on color-singlet and color-octet contribution. The $\eta_c(2S)$ and $h_c(1P)$ decaying into $p\bar{p}$ have been searched for with 1×10^8 $\psi(2S)$ decays sample at BESIII and no obvious signal has been observed. The upper limit of the BFs are set to be 3.0×10^{-3} and 1.5×10^{-4} , respectively. With the larger $\psi(2S)$ data sample of 3×10^9 , we could find the evidence of them with the assumption that the efficiency is about 40% and there is no background.

8. Dalitz plot analysis of $\eta_c(1S) \rightarrow K^+K^-\eta$, $\eta_c(1S) \rightarrow K^+K^-\pi^0$, $\eta_c(1S) \rightarrow K^+K^-\eta'$, $\eta_c(1S) \rightarrow \pi^+\pi^-\eta'$ and $\eta_c(1S) \rightarrow \pi^+\pi^-\eta$, in order to investigate the light meson spectroscopy in which scalar mesons remain a puzzle with the reason that they have complex structure, and there are too many states to be accommodated within the quark model without difficulty [140]. Decays of the $\eta_c(1S)$ provide a window on light meson states. A series of related work has been carried out with two photons processes by BABAR [141]. The world's largest $J/\psi(1S)$ data sample of $N_{J/\psi(1S)} = (10087 \pm 44) \times 10^6$ at BESIII provides the good chance for this topic via the M1 transition $J/\psi(1S) \rightarrow \gamma\eta_c(1S)$.

ACKNOWLEDGMENTS

This work is supported in part by the National Natural Science Foundation of China (11605042), basic research plan for key scientific research projects of higher education institutions in Henan Province (21A140012), cultivation Fund for National scientific research projects of Henan Normal University (2021PL07), excellent Youth Foundation of Henan Province (212300410010), the youth talent support program of Henan Province (ZYQR201912178), the National Natural Science Foundation of China (11875122), and the Program for Innovative Research Team in University of Henan Province (19IRTSTHN018).

[1] M. Ablikim *et al.*, Chin. Phys. C, **44**(4): 040001 (2020).
[2] R. Partridge *et al.*, Phys. Rev. Lett. **45**, 1150 (1980).
[3] P.A. Zyla *et al.* (Particle Data Group), Prog. Theor. Exp. Phys. **2020**, 083C01 (2020).
[4] S. K. Choi *et al.*, (Belle Collaboration) Phys. Rev. Lett. **89**, 102001 (2002).
[5] B. Aubert *et al.*, (BABAR Collaboration) Phys. Rev. Lett. **92**, 142002 (2004),
[6] D. M. Asner *et al.*, (CLEO Collaboration) Phys. Rev.

Let. **92**, 142001 (2004).
[7] B. Aubert *et al.*, (BABAR Collaboration) Phys. Rev. D **84**, 012004 (2011).
[8] B. Aubert *et al.*, (BABAR Collaboration) Phys. Rev. D **72**, 031101 (2005).
[9] K. Abe *et al.*, (Belle Collaboration) Phys. Rev. Lett. **89**, 142001 (2002).
[10] J. Beringer *et al.* (Particle Data Group), Phys. Rev. D **86**, 010001 (2012).

- [11] T. A. Armstrong *et al.*, (E760 Collaboration) Phys. Rev. Lett. **69**, 2337 (1992).
- [12] M. Andreotti *et al.*, (E835 Collaboration) Phys. Rev. D **72**, 032001 (2005).
- [13] S. Dobbs *et al.*, (CLEO Collaboration) Phys. Rev. Lett. **101**, 182003 (2008).
- [14] J. L. Rosner *et al.*, (CLEO Collaboration) Phys. Rev. Lett. **95**, 102003 (2005).
- [15] G. S. Adams *et al.*, (CLEO Collaboration) Phys. Rev. D **80**, 051106 (2005).
- [16] M. Ablikim *et al.*, (BESIII Collaboration) Nucl. Instrum. Methods Phys. Res. Sect. A **614**, 345 (2010).
- [17] M. Ablikim *et al.*, (BESIII Collaboration) Chin. Phys. C, **36**, 915 (2012).
- [18] M. Ablikim *et al.*, (BESIII Collaboration) Chin. Phys. C, **41**, 013001 (2017).
- [19] M. Ablikim *et al.*, (BESIII Collaboration) Chin. Phys. C, **37**, 063001 (2013).
- [20] M. Ablikim *et al.*, (BESIII Collaboration) Chin. Phys. C, **42**, 023001 (2018).
- [21] C. Z. Yuan, arXiv: 2102.12044.
- [22] M. Ablikim *et al.*, (BESIII Collaboration), Phys. Rev. Lett. **111**, 242001 (2013).
- [23] T. Barnes, S. Godfrey and E. S. Swanson, Phys. Rev. D **72**, 054026 (2005).
- [24] S. Godfrey and N. Isgur, Phys. Rev. D **32**, 189 (1985).
- [25] Damir Becirevic and Francesco Sanfilippo, JHEP **01**, 028 (2013).
- [26] G.C. Donald, *et al.*, Phys. Rev. D **86**, 094501 (2012).
- [27] R.M. Baltrusaitis *et al.* (Mark-III Collaboration), Phys. Rev. D **33**, 629 (1986).
- [28] J.Z. Bai *et al.* (BES Collaboration), Phys. Lett. B **555**, 174 (2003).
- [29] D.M. Asner *et al.* (CLEO Collaboration), Phys. Rev. Lett. **92**, 142001 (2004).
- [30] B. Aubert *et al.* (BABAR Collaboration), Phys. Rev. Lett. **92**, 142002 (2004).
- [31] S. Uehara *et al.* (Belle Collaboration), Eur. Phys. J. C **53**, 1 (2008).
- [32] A. Vinokurova *et al.* (Belle Collaboration), Phys. Lett. B **706**, 139 (2011).
- [33] R.E. Mitchell *et al.* (CLEO Collaboration), Phys. Rev. Lett. **102**, 011801 (2009).
- [34] M. Ablikim *et al.*, (BESIII Collaboration), Phys. Rev. Lett. **108**, 222002 (2012).
- [35] M. Ablikim *et al.*, (BESIII Collaboration), Phys. Rev. D **100**, 052012 (2019).
- [36] M. Ablikim *et al.*, (BESIII Collaboration), Phys. Rev. D **86**, 092009 (2012).
- [37] T. Burch *et al.*, Phys. Rev. D **81**, 034508 (2010).
- [38] L. Levkova and C. DeTar, Phys. Rev. D **83**, 074504 (2011).
- [39] T. Kawanai and S. Sasaki, arXiv:1110.0888.
- [40] K.K. Seth, arXiv:0912.2776v1.
- [41] A. Vinokurova *et al.*, (Belle Collaboration), Phys. Lett. B **706**, 139 (2011).
- [42] P. del Amo Sanchez *et al.*, (BABAR Collaboration), Phys. Rev. D **84**, 012004 (2011).
- [43] J. Mandel, The Statistical Analysis of Experimental Data (Dover Publications, New York, 1964).
- [44] S.J. Brodsky and G. P. Lepage, Phys. Rev. D **24**, 2848 (1981).
- [45] M. Ablikim *et al.*, (BES Collaboration), Phys. Rev. D **72**, 072005 (2005).
- [46] Q. Zhao, Phys. Lett. B **636** 197 (2006).
- [47] T. Feldmann, P. Kroll, Phys. Rev. D **62** 074006 (2000).
- [48] Y. Jia and G. D. Zhao, High Energy Phys. Nucl. Phys. **23**, 765 (1999) (in Chinese).
- [49] Q. Wang, X. H. Liu, and Q. Zhao, Phys. Lett. B **711**, 364 (2012).
- [50] H. Q. Zhou *et al.*, Phys. Rev. D **71**, 114002 (2005).
- [51] P. Sun, G. Hao, and C.-F. Qiao, Phys. Lett. B **702**, 49 (2011).
- [52] V.V. Braguta, V.G. Kartvelishvili, Phys. Rev. D **81**, 014012 (2010).
- [53] M. Ablikim *et al.*, (BESIII Collaboration), Phys. Rev. D **95**, 092004 (2017).
- [54] V. L. Chernyak and A. R. Zhitnitsky, Phys. Rep. **112**, 173 (1984).
- [55] M. Anselmino, F. Caruso, and S. Forte, Phys. Rev. D **44**, 1438 (1991).
- [56] M. Anselmino, R. Cancelliere, and F. Murgia, Phys. Rev. D **46**, 5049 (1992).
- [57] M. Anselmino, R. Cancelliere, and F. Murgia, Phys. Rev. D **46**, 5049 (1992).
- [58] F. Murgia, Phys. Rev. D **54**, 3365 (1996).
- [59] M. Anselmino, M. Genovese, and D. E. Kharzeev, Phys. Rev. D **50**, 595 (1994).
- [60] R. G. Ping, B. S. Zou, and H. C. Chiang, Eur. Phys. J. A **23**, 129 (2005).
- [61] Y. J. Zhang, G. Li, and Q. Zhao, Phys. Rev. Lett. **102**, 172001 (2009).
- [62] X. H. Liu and Q. Zhao, Phys. Rev. D **81**, 014017 (2010).
- [63] X. H. Liu and Q. Zhao, J. Phys. G **38**, 035007 (2011).
- [64] C. H. Wu *et al.*, (Belle Collaboration), Phys. Rev. Lett. **97**, 162008 (2006).
- [65] M. Ablikim *et al.*, (BESIII Collaboration), Phys. Rev. D **86**, 032008 (2012).
- [66] M. Ablikim *et al.*, (BESIII Collaboration), Phys. Rev. D **87**, 012003 (2013).
- [67] M. Ablikim *et al.*, (BESIII Collaboration), Phys. Rev. D **101**, 012003 (2019).
- [68] M. Ablikim *et al.*, (BESIII Collaboration), Chin. Phys. C **39**, 093001 (2015).
- [69] Walaa I. Eshraim and Christian S. Fischer, Eur. Phys. J. A **54**, 139 (2018).
- [70] M. Ablikim *et al.*, (BESIII Collaboration), Phys. Rev. D **103**, 012009 (2021).
- [71] Kwong *et al.*, Phys. Rev. D **37**, 11 (1988).
- [72] M. Ablikim *et al.*, (BESIII Collaboration), Phys. Rev. D **87**, 032003 (2013).
- [73] C. Jarlskog and E. Shabalin, Phys. Scr. **T99**, 23 (2002); E. Shabalin, *ibid.* **T99**, 104 (2002).
- [74] M. Ablikim *et al.*, (BES Collaboration), Eur. Phys. J. C **45**, 337 (2006).
- [75] M. Ablikim *et al.*, (BESIII Collaboration), Phys. Rev. D **84**, 032006 (2011).
- [76] M. Ablikim *et al.*, (BESIII Collaboration), Phys. Rev. D **96**, 112008 (2017).
- [77] D.J. Gross, S. B. Treiman, and F. Wilczek, Phys. Rev. D **19**, 2188 (1979).
- [78] P. Kroll, Int. J. Mod. Phys. A **20**, 331 (2005).
- [79] K. Gao, arXiv:0909.2812[hep-ex].
- [80] G. Li, Q. Zhao, Phys. Lett. B **670**, 55 (2008).
- [81] T. Peng and B. Ma, Eur. Phys. J. A **48**, 66 (2012).
- [82] D. Cronin-Hennessy *et al.* (CLEO Collaboration), Phys. Rev. D **81**, 052002 (2010).
- [83] C. Edwards *et al.*, (Crystal Ball Collaboration) Phys.

- Rev. Lett. **48**, 70 (1982).
- [84] C. Z. Yuan, Ph.D thesis, Institute of High Energy Physics, Chinese Academy of Sciences, 1997.
- [85] C. Z. Yuan, Mod. Phys. Lett. A **35**, 2030009 (2020).
- [86] M. Ablikim *et al.*, (BESIII Collaboration), Phys. Rev. Lett. **109**, 042003 (2012).
- [87] B. Aubert *et al.*, (BABAR Collaboration), Phys. Rev. D **78**, 012006 (2008).
- [88] M. Ablikim *et al.*, (BESIII Collaboration), Phys. Rev. D **87**, 052005 (2013).
- [89] S. J. Brodsky and G. P. Lepage, Phys. Rev. D **24**, 2848(1981).
- [90] X. H. Liu and Q. Zhao, J. Phys. G **38**, 035007 (2011).
- [91] S. Barsuk, J. He, E. Kou, and B. Viaud, Phys. Rev. D **86**, 034011 (2012).
- [92] F. Murgia, Phys. Rev. D **54**, 3365 (1996).
- [93] K. T. Chao, Y. F. Gu, and S.F. Tuan, Commun. Theor. Phys. **25**, 471 (1996).
- [94] M. Ablikim *et al.*, (BESIII Collaboration), Phys. Rev. D **88**, 112001 (2013).
- [95] S. J. Brodsky and G.P. Lepage, Phys. Rev. D **24**, 2848 (1981); V.L. Chernyak and A.R. Zhitnitsky, Nucl. Phys. **B201**, 492 (1982); Phys. Rep. **112**, 173 (1984).
- [96] Q. Wang, X.H. Liu, and Q. Zhao, arXiv:1010.1343.
- [97] M. Ablikim *et al.*, (BESIII Collaboration), Phys. Rev. D **84**(091102)(R) (2011).
- [98] M. Andreotti *et al.*, (Fermilab E835 Collaboration), Phys. Rev. D **72**, 032001 (2005).
- [99] S. Dobbs *et al.*, (CLEO Collaboration), Phys. Rev. Lett. **101**, 182003 (2008).
- [100] Y. P. Kuang, S. F. Tuan, and T. M. Yan, Phys. Rev. D **37**, 1210 (1988).
- [101] P. Ko, Phys. Rev. D **52**, 1710 (1995).
- [102] For a review, see T. Appelquist, R. M. Baenett, and K. Lane, Annu. Rev. Nucl. Part. Sci. **28**, 387(1978).
- [103] Y. P. Kuang, Phys. Rev. D **65**, 094024 (2002).
- [104] S. Godfrey and J. Rosner, Phys. Rev. D **66**, 014012 (2002).
- [105] J. J. Dudek, R. G. Edwards, and D. G. Richards, Phys. Rev. D **73**, 074507 (2006).
- [106] C. Amsler *et al.*, (Particle Data Group), Phys. Lett. B **667**, 1 (2008).
- [107] See, for example, E. S. Swanson, Phys. Rep. **429**, 243 (2006), and references therein.
- [108] M. Ablikim *et al.*, (BESIII Collaboration), Phys. Rev. Lett. **104**, 132002 (2010).
- [109] J. L. Rosner, Phys. Rev. D **27**, 1101 (1983);
- [110] F. J. Gilman and R. Kauffman, Phys. Rev. D **36**, 2761 (1987); **37**, 3348(E) (1988).
- [111] M. Ablikim *et al.* (BES Collaboration), Phys. Rev. D **73**, 052008 (2006).
- [112] F. Ambrosino *et al.* (KLOE Collaboration), Phys. Lett. B **648**, 267 (2007).
- [113] R. Escribano and J. Nadal, J. High Energy Phys. **05**, 006 (2007).
- [114] F. J. Gilman and R. Kauffman, Phys. Rev. D **36**, 2761 (1987).
- [115] R. N. Cahn and M. S. Chanowitz, Phys. Lett. **598**, 277 (1975); T. F. Walsh, Lett. Nuovo Cimento **14**, 290 (1975).
- [116] M. Ablikim *et al.*, (BESIII Collaboration), Phys. Rev. Lett. **116**, 251802 (2016).
- [117] M. Ablikim *et al.*, (BESIII Collaboration), Phys. Rev. Lett. **105**, 261801 (2010).
- [118] K. Kawarabayashi and N. Ohta, Nucl. Phys. B **175**, 477 (1980).
- [119] K. Kawarabayashi and N. Ohta, Prog. Theor. Phys. **66**, 1789 (1981).
- [120] M. Ablikim *et al.*, (BESIII Collaboration), Phys. Rev. D **99**(072008) (2019).
- [121] M. Ablikim *et al.*, (BESIII Collaboration), Phys. Rev. D **102**(112007) (2020).
- [122] Q.L. Zhang, X. G. Wu, X.C. Zheng, S. Q. Wang, H.B. Fu, and Z. Y. Fang, Chin. Phys. Lett. **31**, 051202 (2014).
- [123] J.Z. Li, Y.Q. Ma, and K. T. Chao, Phys. Rev. D **88**, 034002 (2013).
- [124] H. Fritzsch, M. Gell-Mann, and H. Leutwyler, Phys. Lett. **47B**, 365 (1973).
- [125] Y.-P. Kuang, Front. Phys. China **1**, 19 (2006).
- [126] E. Eichten, S. Godfrey, H. Mahlke, and J.L. Rosner, Rev. Mod. Phys. **80**, 1161 (2008).
- [127] S. Godfrey, J. Phys. Conf. Ser. **9**, 123 (2005).
- [128] Y.-P. Kuang, S.-F. Tuan, and T.-M. Yan, Phys. Rev. D **37**, 1210 (1988).
- [129] P. Ko, Phys. Rev. D **52**, 1710 (1995).
- [130] M. Ablikim *et al.*, (BESIII Collaboration), Phys. Rev. D **97**(052008) (2018).
- [131] M. Ablikim *et al.*, (BESIII Collaboration), Chin. Phys. C, **45**(2): 023002 (2021).
- [132] M.B. Voloshin, Mod. Phys. Lett. A **17**, 1533 (2002).
- [133] J.Z. Bai *et al.*, (BES Collaboration), Phys. Rev. D **62**, 032002 (2000).
- [134] M.B. Voloshin, Phys. Rev. D **74**, 054022 (2006).
- [135] D. Cronin-Hennessy *et al.*, (CLEO Collaboration), Phys. Rev. D **81**, 052002 (2010).
- [136] J.P. Lees *et al.*, (BABAR Collaboration), Phys. Rev. D **86**, 092005 (2012).
- [137] D. M. Asner *et al.*, Int. J. Mod. Phys. A **24**, S1 (2009).
- [138] Y. J. Gao, Y. J. Zhang and Kuang-Ta Chao, arXiv: hep-ph/0701009.
- [139] F. Feng, Y. Jia and W. L. Sang, Phys. Rev. Lett. **115**, 222001 (2015); Phys. Rev. Lett. **119**, 252001 (2017).
- [140] G.'t Hooft, G. Isidori, L. Maiani, A.D. Polosa, and V. Riquer, Phys. Lett. B **662**, 424 (2008); W. Ochs, J. Phys. G **40**, 043001 (2013).
- [141] J.P. Lees *et al.*, (BABAR Collaboration), Phys. Rev. D **89**(112004) (2014); Phys. Rev. D **93** (012005) (2016); arXiv: 2106.05157v1.